Depth-dependence of soil organic carbon additional storage capacity in different soil types by the 2050 target for carbon neutrality

Clémentine Chirol[1,2], Geoffroy Séré[1], Paul-Olivier Redon[3], Claire Chenu[2], Delphine Derrien[4,5]

[1]Université de Lorraine, INRAE, LSE, F-54000 Nancy, France
[2]INRAE, AgroParisTech, Ecologie fonctionnelle et écotoxicologie des agroécosystèmes, Palaiseau, France
[3]Andra, Direction Scientifique & Technologique, Centre de Meuse/Haute-Marne, 55290 Bure, France
[4]INRAE, UMR SAS 1069, L'Institut Agro, Rennes, France
[5]INRAE, Centre de Nancy, Biogéochimie des Ecosystèmes Forestiers, F-54280 Champenoux, France

Correspondence to: Clémentine Chirol (clementine.chirol@inrae.fr)

Abstract. Land planning projects aiming to maximize soil organic carbon (SOC) stocks are increasing in number and scope, often in line with the objective to reach carbon neutrality by 2050. In response, a rising number of studies assess where additional SOC could be stored over regional to global spatial scales. In order to provide realistic values transferrable beyond the scientific community, studies providing targets of SOC accrual should consider the timescales needed to reach them, taking into consideration the effects of C inputs, soil type and depth on soil C dynamics.

This research was conducted in a 320 km^2 territory in North-eastern France where eight contrasted soil types have been identified, characterized and mapped thanks to a high density of fully-described soil profiles. Continuous profiles of SOC stocks were interpolated for each soil type and land use (cropland, grassland or forest). We defined potential targets for SOC accrual using percentile boundary lines, and used a linear model of depth-dependent C dynamics to explore the C inputs necessary to reach those targets within 25 years. We also used values from the literature to model C input scenarios, and provided maps of SOC stocks, maximum SOC accrual and realistic SOC accrual over 25 years.

SOC stocks and maximum SOC accrual are highly heterogenous over the region of study. Median SOC stocks range from 78 - 333 tC ha^{-1}. Maximum SOC accrual varies from 19 tC ha^{-1} in forested Leptosols to 197 tC ha^{-1} in grassland Gleysols. The simulated realistic SOC accrual over 25 years in the whole region of study was five times lower than the maximum SOC accrual. Further consideration of depth-dependent SOC dynamics in different soil types is therefore needed to provide targets of SOC storage over timescales relevant to public policies aiming to approach carbon neutrality by 2050.

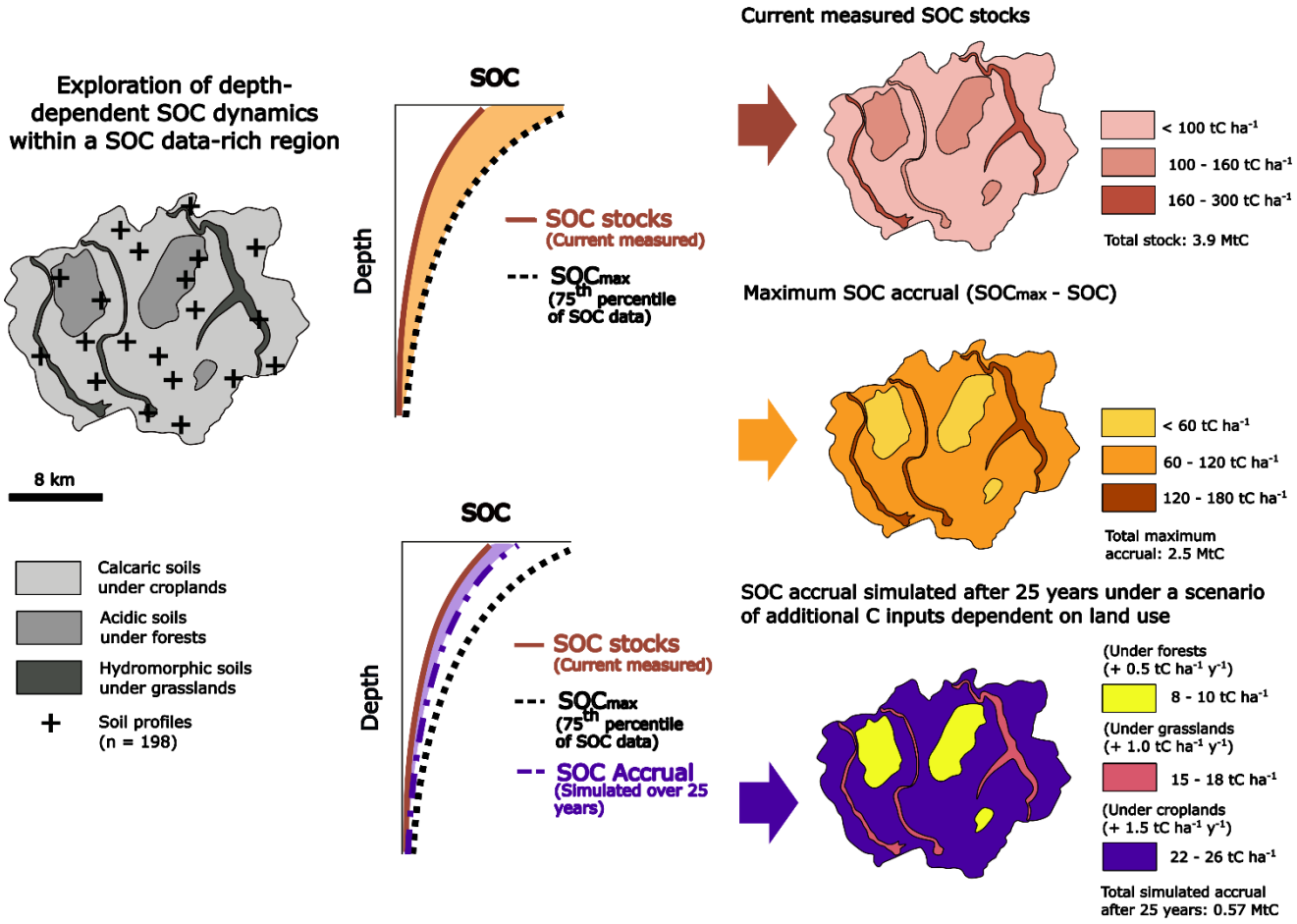

1 Introduction

Soils constitute a carbon reservoir that can help us mitigate for climate change, or conversely accelerate GHG emissions if not managed properly. Objectives for carbon neutrality by 2050 rely on an increase in soil organic carbon (SOC) via changes in land management practices over the coming decades, while preserving existing stocks (Minasny *et al.*, 2017). There is a rising demand for the scientific community to provide quantitative targets for SOC accrual for stakeholders at regional scales and over decadal timescales. However, soils are heterogenous and dynamic systems: soil carbon stocks are constantly being mineralized and renewed by new inputs. The spatial heterogeneity of soil carbon stocks and fluxes presents a challenge to soil carbon sequestration strategies. Certain soils may represent large stocks that need to be preserved, while others may have a greater capacity for SOC accrual.

Estimation of SOC stocks and SOC stock accrual potential should be performed over the whole soil profile because SOC below 20 cm can account for more than 50% of the total stock (Jobbágy & Jackson, 2000; De Vos *et al.*, 2015). Impacts of

management practices on SOC dynamics have been found to vary above and below 30 cm, so the consideration of the whole soil profile is important to provide accurate recommendations to stakeholders (Tautges *et al.*, 2019).

Targets of SOC accrual are currently estimated using two distinct concepts. The first is the fine fraction saturation approach, using the clay and silt content as a proxy of the maximum carbon content that a given soil is theoretically able to stabilize in association with mineral phases (Hassink 1997, Angers *et al.*, 2011). The other is based on the analysis of current ecosystems' functioning: this method seeks the highest observed SOC stock from a dataset taken in a given pedoclimatic context, and assumes this stock to be a realistic target under the management practices captured by the dataset (Lal 2016, Chen *et al.*, 2019). In this study we will adapt this method to define depth-dependent targets as a continuous profile. The fine fraction saturation approach will not be used due to our focus on the whole soil profile: at depth, SOC storage becomes limited by diminishing organic matter inputs, therefore carbon saturation in the fine fraction is unlikely to be a pertinent constraint on maximum SOC accrual (Poeplau *et al.*, 2024).

Targets of SOC accrual need to be evaluated over timescales relevant to stakeholders, keeping in mind in particular the carbon neutrality objective by 2050. Getting the kinetics of SOC accrual necessitates a model-driven approach and scenarios of C inputs to the soil (Barré *et al.*, 2017). Mechanistic models of SOC dynamics such as Millenial (Abramoff *et al.*, 2022) are one option to incorporate the effect of climate change and modifications in management practice, but necessitate a lot of input data, therefore simpler models remain valuable to explore (Derrien *et al.*, 2023; Schimel 2023). For some studies, simple linear models dependent on C inputs have proven to be sufficient to capture respiration patterns across different soils and SOC levels, even though temporal fluctuation in respiration fluxes were not properly represented (Fujita *et al.*, 2014). We will use a linear model that contains a fast cycling, a slow cycling and an inert pool. Pool size and turnover have been calibrated by Balesdent *et al.* (2018) using a global database of C concentrations and 13C isotopes measured after a change in vegetation in multiple campaigns, principally over several decades. This calibration makes the Balesdent *et al.* (2018) parameters singularly robust to estimate C accrual over 25 years.

In addition to land use (Guo & Gifford, 2002), the physico-chemical properties of the soil play an important role on SOC accumulation and residence time (Kögel-Knabner *et al.*, 2021). Soil properties that affect SOC stabilization include the clay content and exchangeable cations (Rasmussen *et al.*, 2018). High Ca^{2+} concentrations in soils were found to intensify SOC accumulation either through increased occlusion within aggregates or through enhanced SOC association with minerals (Rowley *et al.*, 2021). Low pH values also hinder microbial activity and organic matter degradation, leading to an increased residence time of SOC in the soil (Malik *et al.*, 2018). The parameters from Balesdent *et al.* (2018) in the model will therefore be modulated with functions from other models that account for these soil properties. Finally, SOC dynamics are impacted by climate change, both directly through the effects of soil temperature and moisture on C decomposition rates, and indirectly through modifications in soil properties (Luo *et al.*, 2017).

Once targets of SOC accrual have been set for a given timescale, the next step to facilitate communication with stakeholders is to map where this carbon can be stored in a given region, in order to account for the spatial heterogeneity of soils. Soil maps therefore constitute an important tool to spatially assess SOC stocks and fluxes (Wiesmeier *et al.*, 2015).

The main objective of this paper is to estimate and map realistic targets for SOC accrual within decadal timescales, accounting for soil type and depth. To that end, we will explore the effect of land use and soil type on whole-profile SOC stocks and decadal dynamics. We focus on a region of study where dense data collection has taken place and where land use change has seen very little variation for 200 years. We use a combination of pre-existing methods (interpolation of continuous SOC profiles, estimation of theoretical maximum SOC stocks based on observed values, application of a simple model of C dynamics robust at decadal timescales, mapping of the simulated SOC accrual after 25 years) as an innovative way of generating realistic results that are transferrable beyond the scientific community. We will explore two scenarios of SOC accrual: one where we apply annual C inputs necessary to reach the theoretical maximum SOC stock within 25 years, and one where we apply realistic C input values found in the literature. We will also explore scenarios with different rates of temperature increase by 2050 following climate change scenarios RCP4.5 and RCP8.5.

2 Materials and Methods

2.1 Study site and data acquisition

The Perennial Observatory of the Environment (OPE in French) is monitoring since 2007 a 320 km^2 area located in the North-Eastern part of France (in Meuse and Haute Marne counties). This observatory operated by the Radioactive Waste Management Agency (ANDRA) aims to follow the environmental impacts of a planned deep underground nuclear waste storage facility. In the framework of the monitoring program, various environmental data including soil characterization and mapping have been collected.

The OPE study area is dominated by agricultural and forest lands: 55% of the region is occupied by agricultural lands managed by conventional agriculture practices; 29% is occupied by forests dominated by deciduous trees (oak, charm, beech); 14% is occupied by grassland, and less than 2% by urban areas. A land occupation map from 1830 shows that limited modifications in land use have taken place over the past 200 years (Dupouey *et al.*, 2008). The region's continental climate is softened by some oceanic influences. According to data collected by the OPE weather stations from 2009 to 2019, the mean annual temperature is 10.4 °C (+/- 6.2 °C between summer and winter), annual cumulated rainfall is 983 mm (+/- 113) and ETP = 661 mm (+/- 79).

This study uses a total of 198 soil profiles (932 samples) to estimate SOC stocks and maximum SOC accrual. 86 of these soil profiles were collected within the region of study between 1995 and 2019, and were used along with a 1/50,000 pedological map (Party *et al.* / Sol Conseil 2019) to classify the soils into eight dominant soil types and define the physico-chemical characteristics of each of their horizons, such as pH, $CaCO_3$, texture and rock fragment content (Table 1).

The eight identified soil types can be broadly divided based on the geological parent materials and the geomorphology of the region (Figure 1). On the plateaus, preserved detritic Cretaceous layers from the Valanginian stage with high concentrations of silt and sand lead to the formation of Eutric and Dystric Cambisols, with locally Podzosols reaching deeper than 2 m. On the hillslopes and in the valleys, the parent materials are Tithonian limestones and Kimmeridgian marls and limestones, leading

to the formation of Calcaric to Hypereutric Cambisols with high rock fragment contents in the deeper horizons. Soils on the hillslopes, referred to as Rendzic Leptosols and Hypereutric Epileptic Cambisols, are more superficial and have higher rock fragment contents. Stagnosols and Gleysols can be found at the bottom of the valleys and over the Kimmeridgian marls and limestones: they are deep, clay-rich and hydromorphic soils; the former is waterlogged for part of the year while the latter is waterlogged all year round. In the north-east of the study area, clay-rich and $CaCO_3$-bearing materials from a tunnel excavation in 1841-1846 form local pockets of Technosols, which were not considered in this study due to their limited spatial extent. Land use information was derived from the 1/100,000 CORINE Land Cover 2018 at a resolution of 25 ha.

The data from the 86 soil profiles contain SOC content data in the different soil horizons (253 samples), but only 48 bulk density measurements using the cylinder method. In order to provide additional SOC content and bulk density data as a function of depth, 112 additional profiles corresponding to these eight soil types were collected from soil databases in the six surrounding administrative geographical units (counties). The soil profiles were collected by the RMQS (French Soil Quality Monitoring Network) and Renecofor (French Permanent Plot Network for the Monitoring of Forest Ecosystems). In each collected sample, organic carbon content (g kg^{-1}) is measured in the fine fraction (< 2 mm) by dry combustion after removal of the inorganic carbon with acid. Since this study only considers mineral soil, the litter layer was excluded from the forest profiles. Bulk density values are measured using the cylinder method in 552 out of the 932 samples, and are otherwise estimated from a pedotransfer function from Beutler *et al.* (2017) based on clay and total organic content values as follows:

$$BD = [1.6179 - 0.0180 * (Clay + 1)^{0.46} - 0.0398 * SOC^{0.55}]^{-1.33} \quad (1)$$

where BD is the bulk density (kg m^{-3}), Clay is the clay content (g kg^{-1}), and SOC is the total organic carbon content (g kg^{-1}). The pertinence of this pedotransfer function to estimate bulk density in our region of study has been validated with the 48 samples from the region of study where bulk density measurements were available with a mean square error value of 0.70. Other pedotransfer functions from the literature (Saxton & Rawls, 2006; Akpa *et al.*, 2016; Shiri *et al.*, 2017) were also tested but gave mean square error values of 3.13, 6.81 and 353.35 respectively.

Table 1: Mean values of pH, clay content, rock fragments content and $CaCO_3$ concentration for each soil type and horizon, calculated from 86 whole soil profiles sampled between 1995 and 2019 within the region of study. Standard deviations are given in brackets. See measurement protocols in Appendix A.

Soil Type	Horizon	Depth (cm)	Horizon Thickness (cm)	Clay (g kg^{-1})	pH	Rock fragments (%)	$CaCO_3$ (g kg^{-1})
Calcaric Rendzic Leptosols	1	35 (9)	16 (5)	478 (68)	7.8 (0.9)	3 (15)	58 (118)
	2		19 (6)	392 (123)	8.3 (0.4)	35 (30)	414 (186)
Calcaric Cambisol	1	60 (17)	14 (6)	462 (110)	7.8 (0.9)	8 (15)	13 (136)
	2		21 (11)	394 (87)	8.2 (0.4)	35 (23)	465 (250)
	3		25 (11)	328 (110)	8.3 (0.3)	70 (20)	389 (246)
Hypereutric epileptic Cambisol	1	43 (11)	22 (7)	489 (73)	7.8 (0.8)	0	0
	2		21 (5)	523 (86)	6.9 (1.1)	60 (31)	0
Hypereutric Cambisol	1	84 (61)	20 (6)	409 (125)	6.9 (1.0)	2 (13)	0
	2		30 (14)	522 (147)	7.5 (0.7)	3 (28)	0
	3		33 (45)	733 (119)	7.8 (0.4)	50 (26)	2 (5)
Eutric Cambisol	1	85 (30)	18 (6)	278 (107)	5.6 (0.8)	0	0
	2		27 (10)	484 (164)	6.2 (1.0)	0	0
	3		40 (28)	595 (207)	7.5 (1.5)	5 (36)	2 (17)
Dystric Cambisol	1	168 (33)	15 (5)	40 (1)	4.0 (0.2)	0	0
	2		18 (3)	27 (6)	4.3 (0.2)	0	0
	3		10 (0)	40 (8)	4.3 (0.2)	0	0
	4		48 (3)	75 (9)	4.7 (0.1)	0	0
	5		78 (23)	95 (44)	4.6 (0.1)	0	0
Stagnosol	1	115 (30)	28 (5)	490 (182)	7.8 (1.0)	0	2 (196)
	2		40 (11)	353 (131)	8.2 (1.4)	0	98 (244)
	3		47 (11)	346 (111)	8.4 (1.2)	1 (15)	576 (236)
Gleysol	1	140 (41)	23 (7)	453 (88)	7.8 (0.4)	0	103 (105)
	2		46 (12)	386 (62)	8.2 (0.3)	0	143 (189)
	3		72 (36)	350 (75)	8.2 (0.3)	0	290 (288)

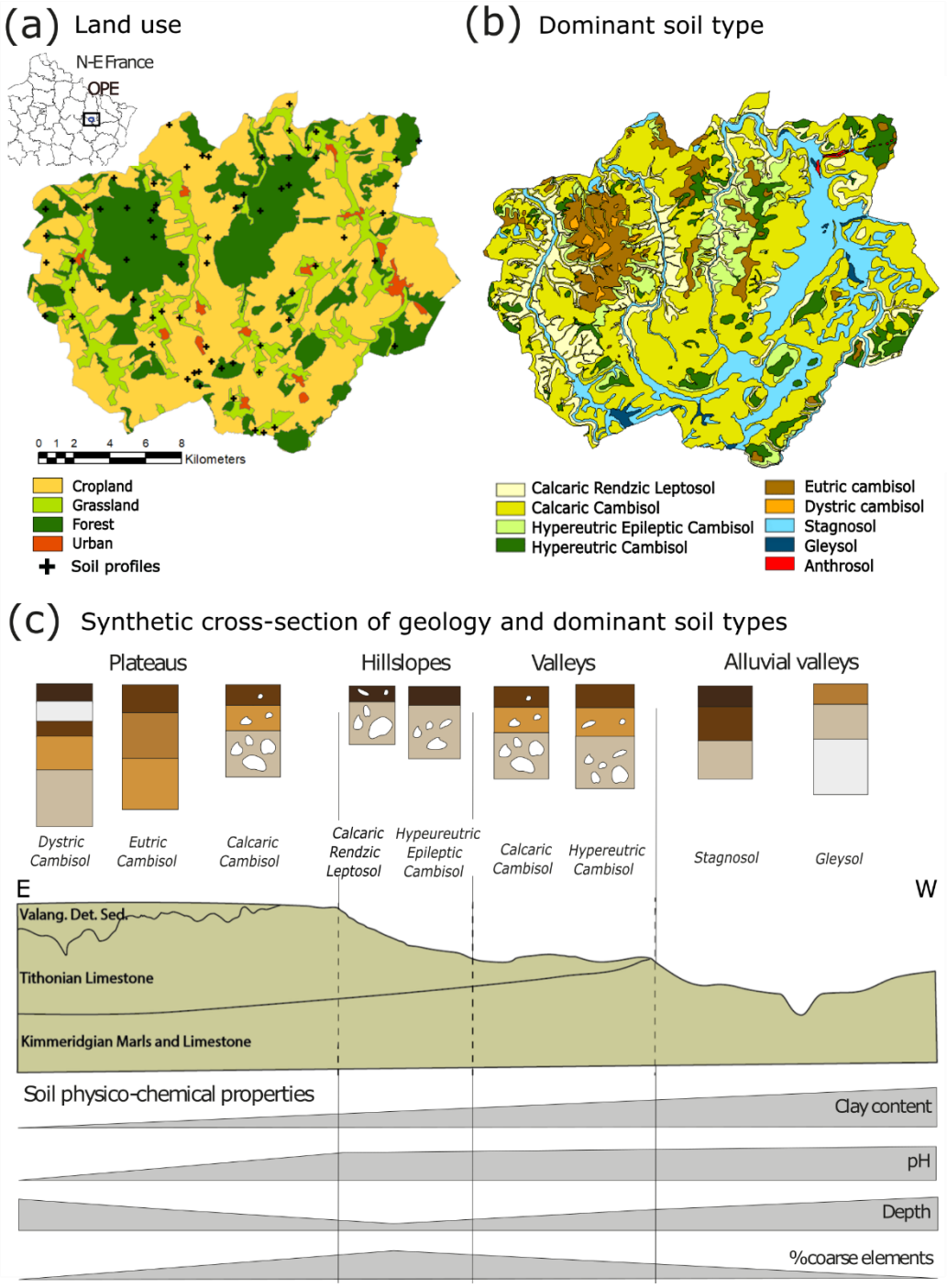

135

Figure 1: Land uses, soil types and geomorphological context of the study region. (a) Land use (Source: Corine Land Cover 2018). (b) Map of dominant soil types (Source: Party *et al.*, 2019). (c) Synthetic cross-section of the geology, topography and dominant soil types in the region of study.

2.2 Estimation of initial and maximum SOC stocks

2.2.1 Initial SOC stocks

Soil organic carbon stocks per surface unit are calculated as follows (Chen *et al.*, 2019):

$$\mathrm{SOCstock} = \frac{\mathrm{p} * \mathrm{SOC} * \mathrm{BD} * (100 - \%\ \mathrm{Rock\ fragments})}{1000} \quad \textbf{(2)}$$

where SOC_{stock} is the total SOC stock (kg m^{-2}), p is the soil thickness (m), SOC the soil organic carbon content (g kg^{-1}), BD the bulk density (kg m^{-3} = g dm^{-3}) and % Rock fragments the percentage of elements > 2 mm (%).

This methodology assumes that the fraction > 2 mm does not contain organic carbon, which has been disputed by Harrison *et al.* (2011) in cases where the rock fragments are abundant and display signs of porosity and weathering.

The median soil organic carbon content (SOC in g kg^{-1}) as a function of depth for each soil type and land use was calculated using the typical SOC content profile established by Mathieu *et al.* (2015) and Jreich (2018) on the basis of three descriptors: Ω_1 the SOC content of the soil type at maximal depth, Ω_2 the SOC content at the surface, and Ω_3 the depth at half maximum of the SOC content:

$$\mathrm{SOC}\,(s, z) = \Omega 1(s) + (\Omega 2(s) - \Omega 1(s)) * e^{-(z/\Omega 3(s))} \quad \textbf{(3)}$$

where *s* is the soil type, *z* the depth.

This method was used to interpolate SOC content data from national and regional datasets, acquired per horizon, in order to obtain the continuous distribution of SOC stock over the whole soil profile for each soil type and land use considered. A least square method for non-linear curve-fitting (Matlab function lsqcurvefit) was then applied to adjust the $\Omega_{1\text{-}3}$ parameters (Appendix B).

Continuous vertical profiles of median bulk density were then obtained for each soil type using a logarithmic fit. The horizon thickness and percentage of rock fragments correspond to the median of the values per horizon per soil types in the 86 profiles within the OPE zone. This gave us a continuous profile of median SOC stocks as a function of depth, corresponding to the initial SOC stock profile. The dataset was collected between 1995 and 2019, but since land use has not changed since 1830, the soil profiles were assumed to be at steady state, and to represent the initial SOC stocks before the implementation of C input modelling scenarios. The median SOC stock was then calculated at each 1 cm interval along the whole profile based on the median bulk density curve, the median SOC curve and the percentage of rock fragments.

2.2.2 Theoretical maximum SOC stocks and maximum SOC accrual

The theoretical maximum SOC stocks in this study are theoretical targets based on the upper values of the SOC data observed within the region. These targets represent the SOC stock that a given soil type can reach under the land management strategies represented in the region of study. The theoretical maximum SOC stock is therefore region-dependent as it is not solely driven by the intrinsic textural properties of the soil, but also by climate and the ecosystem plant productivity as they influence soil biology and chemistry along the soil profile. The maximum SOC accrual corresponds to the difference between the theoretical maximum SOC stock and the initial SOC stock.

The regression fit method applied using equation 3 from Jreich (2018) worked iteratively by first computing the 50th percentile boundary line (median profile corresponding to the initial SOC stocks) and removing all data points inferior to that line. The process was then repeated for the 75th percentile, then the 88.5th, and finally the 94th. The choice in percentile value strongly affects the estimation of maximum SOC stocks (Chen *et al.*, 2019). In our case, since the number of SOC data points per soil type ranges from 29 (Hypereutric Epileptic Cambisol) to 268 (Stagnosol), the 75th boundary line is calculated based on 14 to 134 data points, the 88.5th percentile based on 7 to 67 data points, and the 94th percentile based on 3 to 34 data points. We chose the 75th boundary line to define the theoretical maximum SOC stocks. We also calculated the 88th percentile boundary line to discuss its impact on theoretical maximum stocks and on subsequent SOC dynamic modelling.

A bootstrap method was used to determine the overall uncertainty of the initial SOC stocks and maximum SOC accrual for each soil type at 90% confidence interval (Chen *et al.* 2019). We generated random subsets of input parameters SOC, BD, percentage of rock fragments and depth values within the standard deviation of each soil type, and repeated the procedure 1000 times to obtain 1000 estimates of the mean and percentiles values of the carbon stocks.

2.3 Simulation of SOC accrual at different timescales

Our modelling approach is illustrated in Figure 2, with further details of model functioning and equations in Appendix C. The profiles of initial SOC stocks were first discretized into 10 cm layers. In each layer, we applied a three-pool model with a fast cycling, a slow cycling pool and an inert pool, where the dynamic pools are ruled by exponential kinetics. SOC stocks do not saturate and are linearly dependent on C inputs for a given situation. Pools relative size and turnover were calibrated by Balesdent *et al.* (2018) using a global database of change in stable carbon (C3/C4) signatures measured over multiple campaigns, over decadal timescales, for 112 grassland, forest and cropland sites. The C3/C4 approach is typically efficient to follow carbon dynamics over timescales ranging from one to one thousand years, especially compared to the ^{14}C method, which covers timescales of several thousand years (Verma *et al.*, 2017). We corrected the model parameters calibrated at the global scale in Balesdent *et al.* (2018) to account for local conditions of temperature, humidity, pH, clay content and $CaCO_3$ content as recommended by Rasmussen *et al.* (2018). This was done using the equations from the AMG model (Andriulo *et al.*, 1999; Saffih-Hdadi & Mary, 2008; Clivot *et al.* 2017; Levavasseur *et al.*, 2020). The mean residence times as a function of depth derived from the corrected mineralization factors in the fast and slow pools can be found in Appendix D.

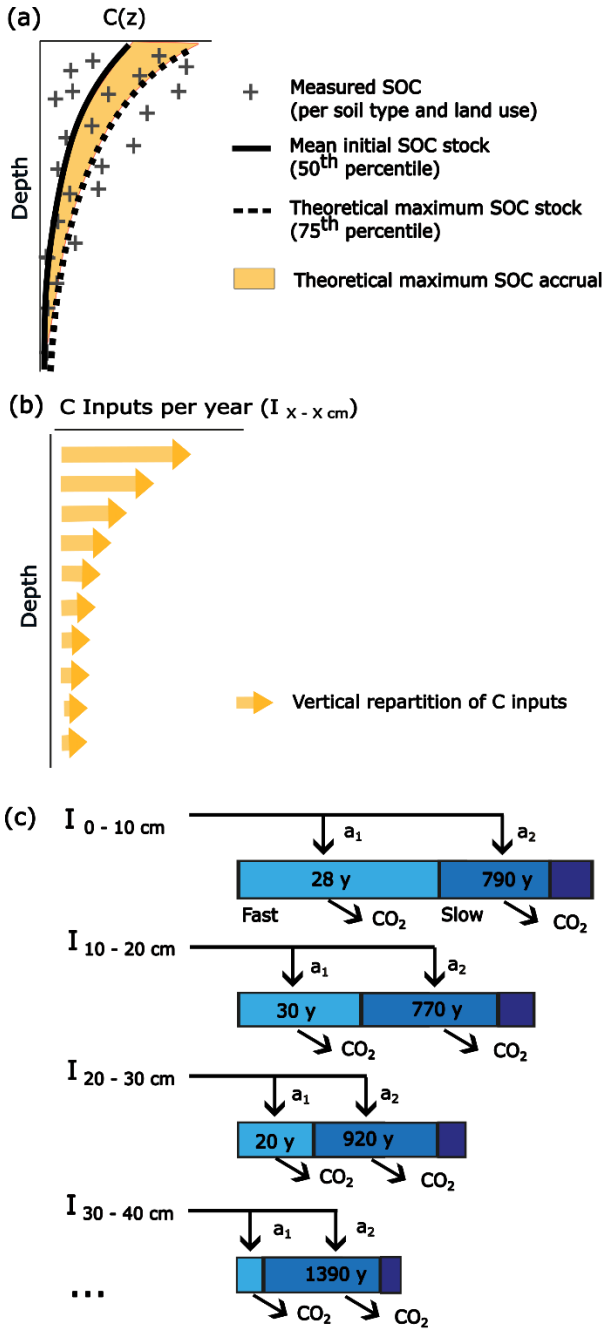

Figure 2: Summary of our approach: (a) estimation of initial and theoretical maximum SOC stocks from the measured data; (b) estimation of vertical repartition of C inputs for the different scenarios considered, obtained by matrix inversion; (c) Functioning of the depth-dependent three-pool model (fast-cycling pool, slow-cycling pool, inert pool). a = allocation factor; MRT = Mean Residence Time (in years), y = years. MRT values vary with depth as per Balesdent *et al.* (2018) and are corrected for temperature, humidity, pH, texture and CaCO3; values displayed correspond to the mean MRT values per pool and depth section (see Methods for details and Appendix D for MRT values for each soil type and depth). The initial C inputs and maximum C inputs are provided in Appendix E.

We modelled three different scenarios of C inputs to explore how much SOC might accrue after 25 years:

- *Scenario 1 (initial input regime)* corresponds to the annual C inputs necessary to maintain the initial SOC stocks in each soil type and land use, obtained by matrix inversion (Mao *et al.*, 2019): there is no SOC accrual in this case;
- *Scenario 2 (extreme input regime)* corresponds to the annual C inputs necessary to reach the theoretical maximum SOC stocks within 25 years, obtained through iterative optimization of the model;
- *Scenario 3 (realistic increased input regime)* defines C inputs values higher than in scenario 1 that are compatible with the ranges of gain in C inputs after implementation of practices promoting C sequestration found in the literature: +0.5 tC ha^{-1} y^{-1} in forests, +1.0 tC ha^{-1} y^{-1} in grasslands, and +1.5 tC ha^{-1} y^{-1} in croplands.

For scenario 3, we sought values of typical current plant inputs and of realistic increased inputs from the literature or from existing data within the region of study. Typical current C inputs in forests range within 1.6 - 2.8 tC ha^{-1} y^{-1} according to measurements carried out in the Renecofor network in the region of study, assuming 50% mineralisation of above ground input in the forest floor (Mao *et al.*, 2019). Changes in harvest practices towards non-export of harvest residues after thinning could provide additional inputs in the range of 0.5 – 2 tC ha^{-1} y^{-1} (total realistic input range: 1.6 – 4.8 tC ha^{-1} y^{-1}) (Mao *et al.*, 2019). In grasslands, annual inputs to the soil range within 1.18 – 5.2 tC ha^{-1} y^{-1} according to studies from Australia and Western Europe (methods used: RothC inverse modelling, allometric equations using yield data, expert opinion) (Martin *et al.*, 2021). In croplands, annual inputs to the soil range within 1.8 – 6.8 tC ha^{-1} y^{-1} according to studies conducted worldwide (methods used: direct measurements, RothC inverse modelling, allometric equations using yield data, expert opinion) (Martin *et al.*, 2021). Within these ranges, the specific realistic values for the region of study were chosen by matrix inversion of the theoretical maximum SOC stocks, which provide the annual inputs necessary for the model to reach but to not exceed the maximum SOC stocks in the long term.

The equations of SOC stock evolution over time were then applied for these scenarios over 5000 years to visualize the new steady state and assess the maximum potential for C storage. Particular attention was given to the SOC accrual reached after 25 years to fit with the carbon neutrality timeline.

Finally, we tested the effect of projected rises in temperature on the simulated SOC accrual by modifying the mineralization correction factor linked to temperature (see Equation C1). The temperature was increased linearly to projected annual temperatures in the region of study according to the scenarios RCP4.5 (+1.0°C) and RCP8.5 (+1.3 °C) according to model simulations by the Meteo France ALADIN63_CNRM-CM5 model within an 8 km radius area around Bure (55087), comparing the year intervals 2046-2055 and 2009-2019 (Drias, données Météo-France, CERFACS, IPSL). This corresponds to an increase in mean annual temperatures from 10.4 °C to 11.4°C (RCP4.5) or 11.9°C (RCP8.5) over 25 years at all depths. RCP8.5 amounts to an extreme scenario in terms of increased mineralization rates, since in addition to using the most pessimistic RCP scenario,

our model assumes that rises in temperature propagate instantly at depth and that humidity conditions remain at the present levels. We tested the sensitivity of SOC accrual to the two temperature scenarios in the different soil types and land covers.

2.4 Spatialization

The study site was divided into zones characterized by their land use (cropland, grassland, forest) and by their dominant soil type. Mapping zones were derived from the intersection of the CORINE Land Cover map and of the soil map. Values of SOC stocks, maximum SOC accrual, and simulated accrual after 25 years were then associated to each mapping zone.

Mapping results are by necessity a simplification of the real distribution of soils properties and SOC contents. Figure 1b shows the dominant soil type in each mapping zone, but in reality, due to the high spatial variability of soil characteristics, each mapping zone contains several soil types that cannot be explicitly delimited on the map at this spatial resolution. Therefore, each point within a given zone has a probability of belonging to one of several soil types (e.g.: 70% chance of being a Eutric Cambisol, 30% chance of being a Stagnosol). The total SOC stock for a zone is then obtained by the weighted mean of the SOC stocks (e.g. 70 % of the SOC stock for Eutric Cambisols and 30 % of the SOC stock for Stagnosols). The standard deviation of the total SOC stock should likewise be obtained by the weighted standard deviations of the SOC stocks. The local uncertainty corresponds to expected local variations in the zone if the different soil types have contrasted SOC stocks. We visualized this local uncertainty by mapping the contrasts in SOC stocks within each zone in Appendix F.

3 Results

3.1 SOC stock and maximum SOC accrual as a function of depth, land use and soil type

3.1.1 Vertical repartition of SOC stocks

Current SOC stocks over the whole profile range from 78 to 333 tC ha^{-1} (Table 2), of which 59 to 156 tC ha^{-1} are in the topsoil (0 - 30 cm). The lowest SOC stocks are found in the shallower soil types (Calcaric Rendzic Leptosol and Hypereutric Epileptic Cambisol). Current SOC stocks are twice to three times higher in hydromorphic soils (Stagnosols and Gleysols) compared to non-hydromorphic soils.

SOC content and stocks decrease with depth, with sharp decreases in the SOC stock profiles corresponding to a change in the percentage of rock fragments between two horizons (Figure 3). On average, excluding the shallower soil types (Calcaric Rendzic Leptosol and Hypereutric Epileptic Cambisol), the proportion of the SOC stock situated in the first 30 cm is 53 % in croplands, 67 % in grasslands and 71 % in forests (Appendix G). The soils in croplands are therefore depleted in SOC in the topsoil compared to forests and grasslands (Figure 3a). The difference in SOC stocks between land uses diminishes in the deeper horizons.

Table 2: Initial SOC stocks, C input regimes to the soil considered in this study, theoretical maximum SOC stocks based on the 75th percentile of our regional dataset, and SOC stock after 25 years under a realistic scenario of C inputs, for each soil type and land use. Realistic range of annual C inputs to the soil is 1.8 – 6.8 tC/ha/y for croplands (Martin *et al.*, 2020), 1.18 – 5.2 tC/ha/y for grasslands (Martin *et al.*, 2020), and 1.6 – 4.8 tC/ha/y for forests according to measurements made in the region of study.

Depth (cm)		Initial SOC stock (90% confidence interval in brackets) (tC ha^{-1})	Theoretical maximum SOC stock (75th percentile) (tC ha^{-1})	Scenario 1: Initial input regime (tC ha^{-1} y^{-1})	Scenario 2: Extreme input regime (tC ha^{-1} y^{-1})	Scenario 3: Realistic increased input regime (tC ha^{-1} y^{-1})	SOC stock after 25 years under realistic increased input regime (tC ha^{-1})
Calcaric rendzic leptosol	C	78 *(48-115)*	167	1.3	7.0	2,8	102
	G	101 *(84- 138)*		1.9	6.0	2,9	118
	F	149 *(97- 183)*		2.7	3.8	3,2	157
Calcaric cambisol	C	100 *(58- 133)*	191	1.8	7.9	3,3	123
	G	134 *(66- 183)*		2.7	6.5	3,7	150
	F	148 *(104- 184)*		2.8	5.7	3,3	156
Hypereutric epileptic cambisol	C	92 *(49- 129)*	129	1.5	3.8	3	117
	F	106 *(76- 121)*		2.0	3.4	2,5	115
Hypereutric cambisol	C	103 *(62- 137)*	228	1.4	9.5	2,9	127
	G	167 *(125- 255)*		2.5	6.4	3,5	183
	F	160 *(92- 204)*		2.3	6.7	2,8	168
Eutric cambisol	C	102 *(59- 144)*	194	1.0	6.4	2,5	128
	G	90 *(66- 115)*		1.2	7.4	2,2	107
	F	157 *(71- 190)*		2.0	4.2	2,5	166
Dystric cambisol	F	120 *(76- 198)*	169	1.0	3.7	1,5	129
Stagnosol	C	166 *(101- 237)*	285	1.5	9.2	3	189
	G	161 *(108- 279)*		1.9	9.8	2,9	177
	F	172 *(121- 249)*		2.3	9.4	2,8	181
Gleysol	C	279 *(154- 417)*	476	2.8	17.3	4,3	301
	G	333 *(252- 466)*		4.6	14.9	5,1	349

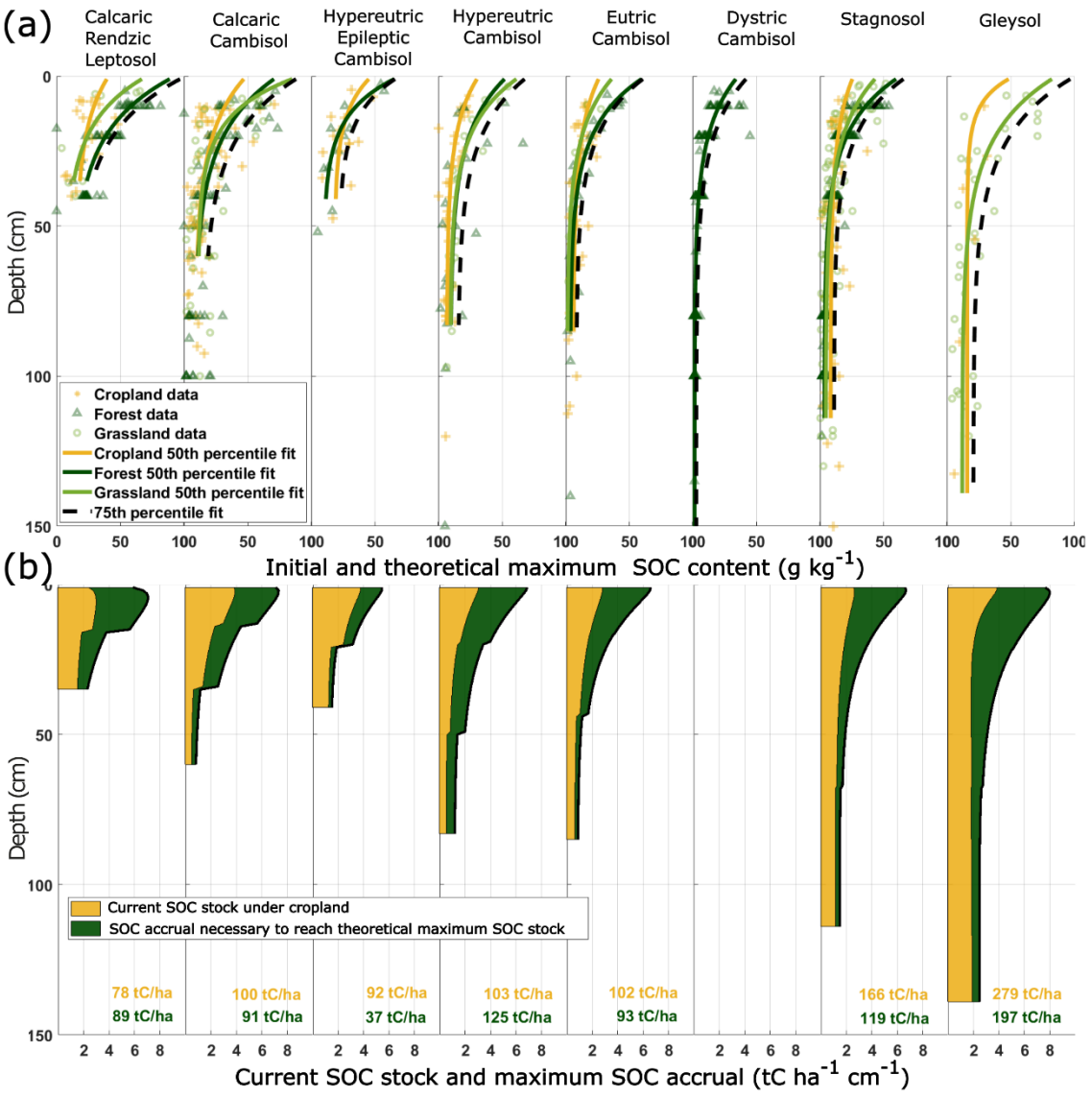

Figure 3: (a) Median (50th percentile of the dataset for each land use) and theoretical maximum (75th percentile of the dataset) fitted depth profiles of SOC content in each soil type. The Jreich parameters (2018) used to plot the SOC content profiles are given in Appendix B. (b) Current SOC stocks under croplands and maximum SOC accrual to reach the theoretical maximum SOC stocks of each soil type.

3.1.2 Theoretical Maximum SOC stocks and maximum SOC accrual

The theoretical maximum SOC content decreases with depth under all soil types, from 50-100 g kg^{-1} near the surface to under 25 g kg^{-1} at the bottom of the soil profiles (Figure 3a). The theoretical maximum SOC stocks range from 129 tC ha^{-1} in the Hypereutric Epileptic Cambisol to 476 tC ha^{-1} in the Gleysols.

The maximum SOC accrual varies from 19 tC ha^{-1} for shallow, rocky forest soils to 197 tC ha^{-1} for agricultural Gleysols considering a conversion of cropland into grassland or forest. According to the 75th percentile method, soils in the region of study are at 74% of their theoretical maximum SOC stock on average, ranging between 16-61% for croplands, 30-56% grasslands and 40-82% for forests. Across all land uses, the shallow rocky soils (Calcaric Rendzic Leptosol and Hypereutric Epileptic Cambisol) are closer to their theoretical maximum SOC stocks than the Stagnosols and Gleysols. Using percentile 88th instead of 75th increases our estimation of the theoretical maximum SOC stocks by about 16% (9 - 27% depending on soil type), without changing the hierarchy of tmaximum SOC stocks across the eight soil types (Appendix G).

3.2 Exploring kinetics of simulated SOC accrual

The equations of our model calculate the SOC mean residence times per depth as a function of the physico-chemical properties of the studied soil types (see Equations C1-5). In our study site, they range from 50 – 100 years above 30 cm and from 145 – 453 years below 30 cm (Appendix D). The increase in mean residence time with depth is stark in the slow pool (from 477 – 1100 years in the first 10 cm to 1744 – 5817 years in the deeper soil horizons), but is hardly discernible in the fast pool (17-38 years in the first 10 cm to 11-47 years in the deeper soil horizons). Since most of the new C inputs are allocated to the fast carbon pool and in the surface horizons (Appendix D-E), the SOC accrual is not strongly affected by soil type over 25 years.

The initial stationary C inputs obtained by model matrix inversion are, depending on soil type, between 1.0 – 2.8 tC ha^{-1} y^{-1} for croplands, 1.2 – 4.6 tC ha^{-1} y^{-1} for grasslands and 1.0 – 2.8 tC ha^{-1} y^{-1} for forests (Table 2). By contrast, the extreme input regime needed to reach the theoretical maximum SOC stocks within 25 years ranges between 3.8 - 17.3 tC ha^{-1} y^{-1} for croplands, 6.0 - 14.9 tC ha^{-1} y^{-1} for grasslands and 3.4 - 9.4 tC ha^{-1} y^{-1} for forests. The realistic increased input regime chosen based on the literature is 2.5 – 4.3 tC ha^{-1} y^{-1} for croplands, 2.2 – 5.1 tC ha^{-1} y^{-1} for grasslands and 1.5 – 3.3 tC ha^{-1} y^{-1} for forests.

Under the realistic increased input regime, and when rising temperatures are not considered, the SOC accrual after 25 years ranges from 22-26 tC ha^{-1} under cropland, 15-18 tC ha^{-1} under grassland, to 8-10 tC ha^{-1} under forest (Figure 4, Appendix H). Kinetics of SOC accrual are dependent on the time since the implementation of the practice increasing C inputs to soil. The yearly accrual rates averaged over the first few decades range between 0.88-1.04 tC ha^{-1} y^{-1} under croplands, 0.6-0.72 tC ha^{-1} y^{-1} under grassland and 0.32-0.4 tC ha^{-1} y^{-1} under forest. The accrual rates then decrease over decadal and centennial timescales as the SOC stocks stabilize asymptotically towards the new steady state, as per the model equations. SOC accrual at the new steady state is highest under Dystric Cambisol owing to the effect of the low pH on the mineralization rates as implemented in the model. Modelled SOC accrual after 25 years decreases with depth under all soil types and land uses (Figure 5).

Under the RCP4.5 scenario of 1.0 °C increase over 25 years, the SOC accrual is attenuated by 7 to 38% compared to the SOC accrual simulated at constant temperature (10% under cropland, 20% under grassland and 30% under forest on average). The SOC accrual after 25 years under this scenario ranges from 16-24 tC ha^{-1} under cropland, 10-16 tC ha^{-1} under grassland, to 5-8 tC ha^{-1} under forest (Appendix H).

Incorporating the RCP8.5 scenario of 1.3 °C increase in temperature over 25 years attenuates SOC accrual by 10 to 50%, and shows a stronger impact of soil type and especially land cover on the mineralization rates (Appendix H). SOC accrual is

attenuated by 10-20% in cropland soils, 10-40% in grassland soils, and 40-50% in most forest soils except Dystric Cambisols (20%).

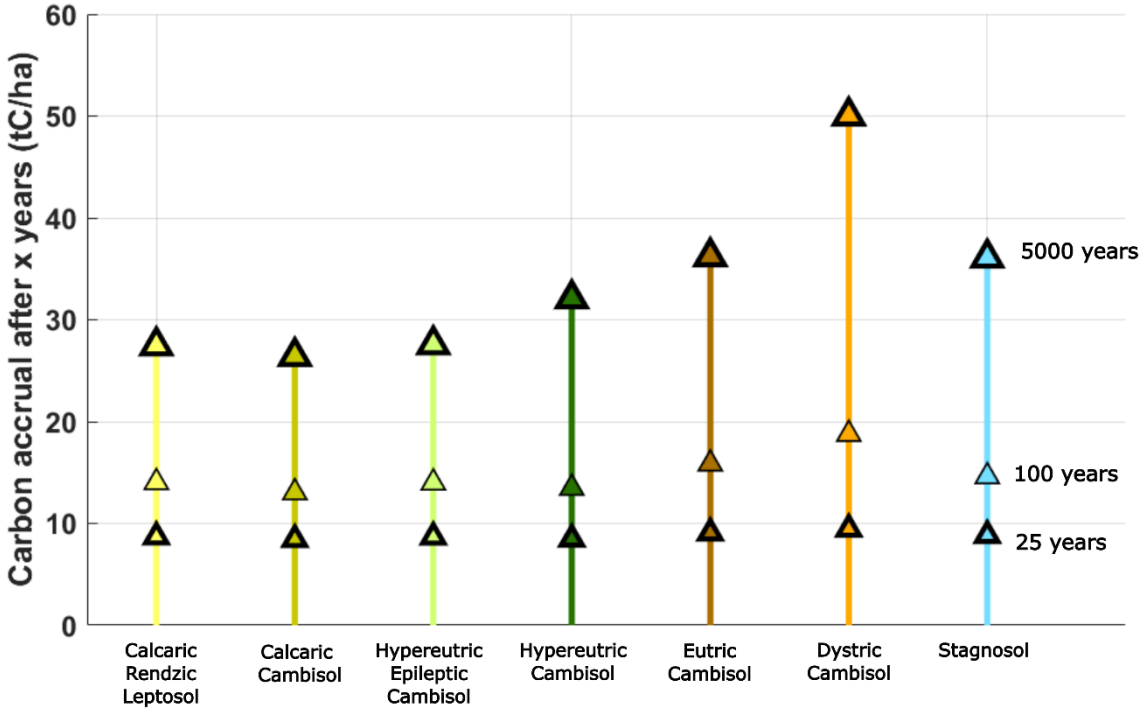

Figure 4: Model results of SOC accrual after 25, 100 and 5000 years under forests for a scenario of +0.5 tC ha^{-1} y^{-1} compared to the initial C inputs, temperature remaining constant.

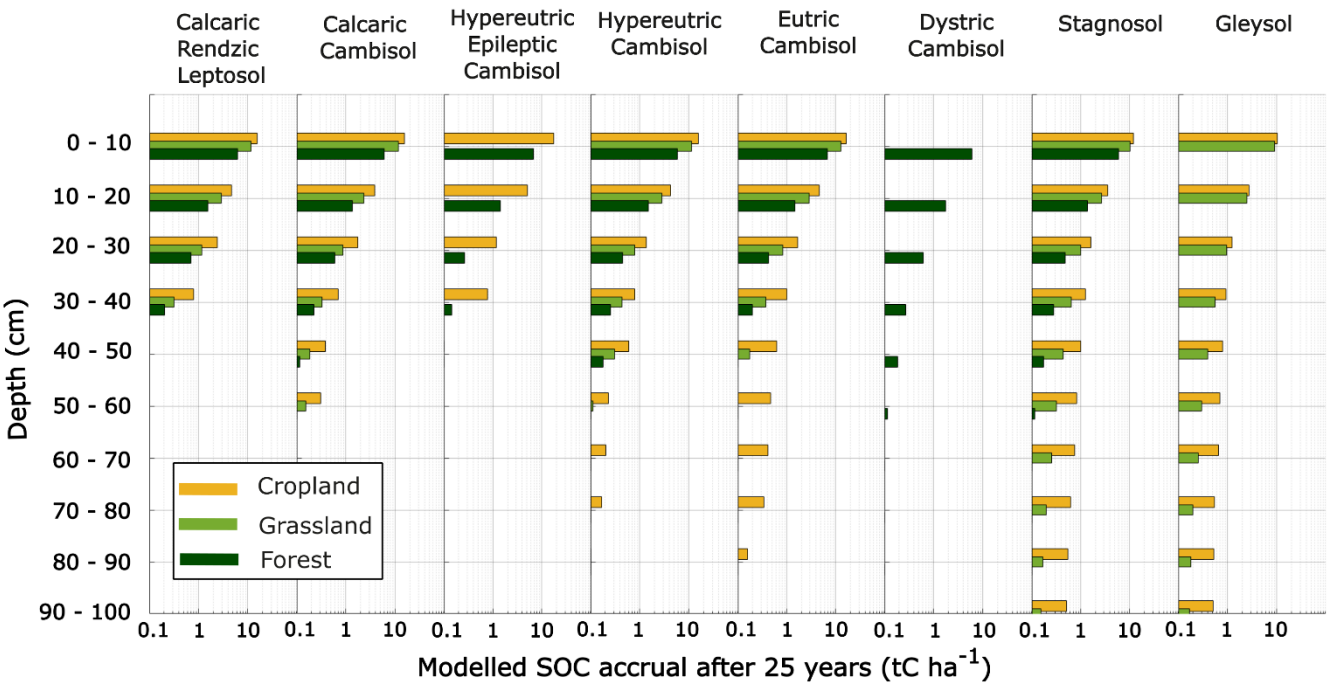

Figure 5: Model results of SOC accrual after 25 years at each depth under the three considered C input scenarios (+1.5 tC ha^{-1} y^{-1} under croplands, +1.0 tC ha^{-1} y^{-1} under grasslands, +0.5 tC ha^{-1} y^{-1} under croplands compared to the initial C inputs), temperatures remaining constant. Model results for each soil type are only shown for the land uses represented in the dataset.

3.3 Maps of SOC stocks, maximum SOC accrual, and simulated accrual after 25 years

The repartition of SOC stocks and maximum SOC accrual in the region of study is most visibly related to land use, but is also affected by the spatial distribution of Stagnosols and Gleysols (Figure 6). The current SOC stock in the region of study amounts to a total of 3.9 MtC, with a standard deviation of 1.5 MtC according to the bootstrap method (Appendix I). To compare these results with national-scale estimates of SOC stocks, we average 3.9 MtC over the entire region of study and obtain a mean value of 122 tC ha^{-1}, of which 87 tC ha^{-1} are in the first 30 cm.

The maximum SOC stocks that the region can theoretically contain is 3.9 + 2.5 = 6.4 MtC, suggesting that the soils in the region of study are at 61% of their theoretical maximum SOC stock. However, according to model results in scenario 3, this maximum SOC stock would only be reached over timescales of centuries to millenia, and the SOC accrual after 25 years only reaches 0.57 MtC. The SOC accrual in the region of study is attenuated by 14% and reaches 0.49 MtC when a 1.0 °C increase in temperature is implemented in the mineralization rates (Appendix J).

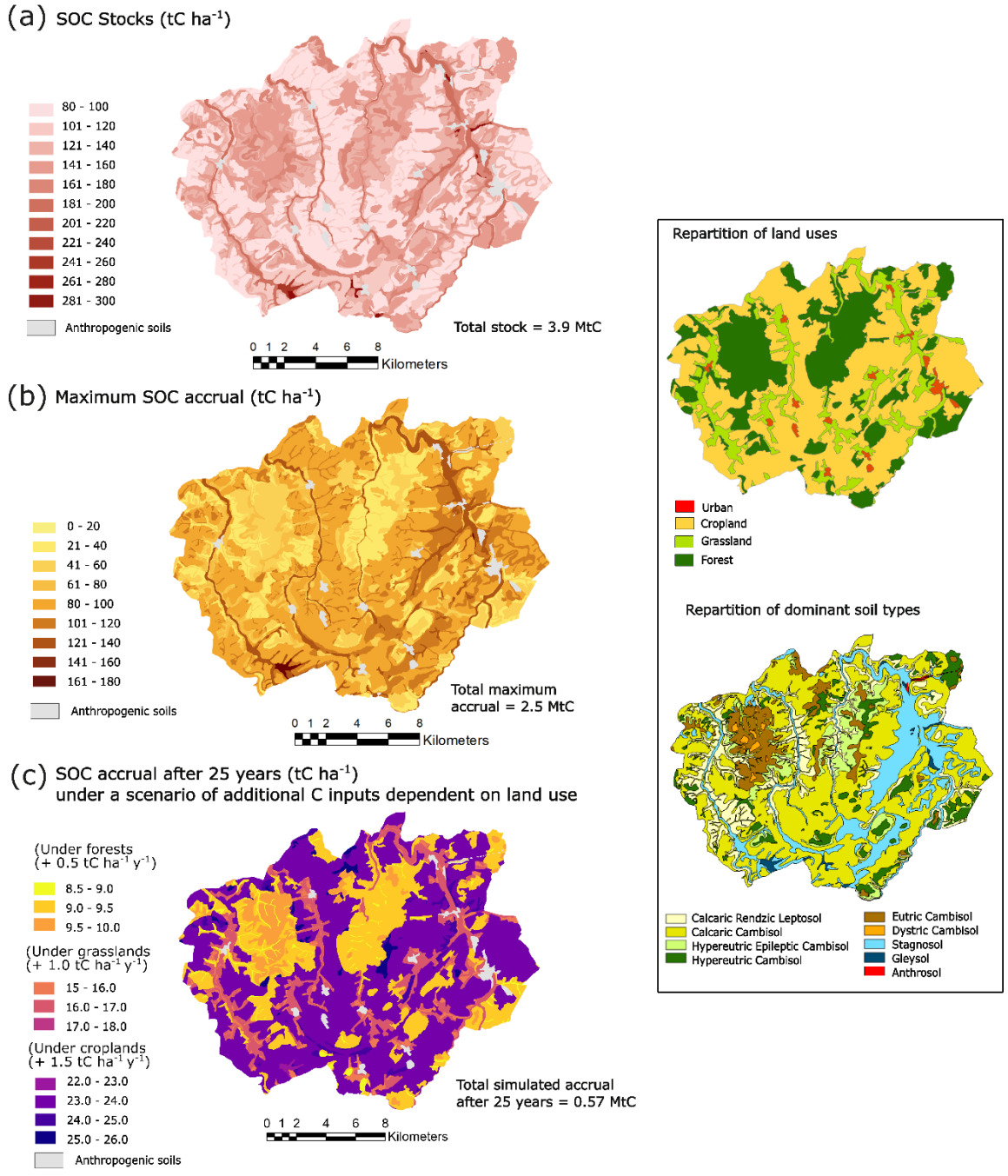

Figure 6: Maps of SOC stocks (a), maximum SOC accrual (b) and simulated SOC accrual after 25 years under a realistic increased input scenario (+ 0.5 tC ha^{-1} y^{-1} under forests, + 1.0 tC ha^{-1} y^{-1} under grassland, + 1.5 tC ha^{-1} y^{-1} under cropland) (c). Upper and lower confidence intervals provided by the bootstrap method are given in Appendix I. The standard deviation of the total SOC stocks and maximum SOC accrual based on the upper and lower confidence intervals applied to the whole region is 1.5 MtC.

4 Discussion

4.1: Implications of our approach to estimate target SOC stocks and accrual rates

There is a rising interest in representing the contribution of soils to carbon storage, both through the mapping of current SOC stocks, and through the mapping of the maximum SOC stocks that these soils can theoretically reach. Modelling can then be used to explore the input rates and timescales needed to reach these targets SOC stocks. Our approach for estimating SOC theoretical maximum stocks was made possible by the uncommon abundance of soil profile data and by the detailed pedological map available in the region of study. This approach is most pertinent in areas where the land use and management has remained stable for many years (over 200 years in our region of study), because the high values of SOC stocks used to estimate target SOC stocks per soil type are more likely to represent a steady state rather than a transient stage. Such data-rich, well-documented regions can serve as references for similar pedoclimatic zones. A further step would then be to intensify profile-scale data collection in other regions to provide reference values of SOC stocks and maximum SOC accrual in as many pedoclimatic zones as possible, in order to upscale this approach from the regional to the global scale (Barré *et al.*, 2017).

Three C input scenarios were implemented to explore kinetics of SOC accrual. The first was an initial input regime obtained by matrix inversion, and corresponds to the annual C inputs necessary to maintain the initial SOC stocks at the steady state. We found a good agreement between the model-derived initial C inputs and available measurements and estimates made within the region of study: in croplands, the simulated C inputs were consistent with estimations of C inputs derived from the method of Bolinder *et al.* (2007) based on crop yields recorded in the region of study (Appendix K). In forests, the model-derived initial C inputs were consistent with measurements from the Renecofor carried out in the region of study.

The second scenario sought the annual C inputs necessary to reach the theoretical maximum SOC stocks within 25 years. The required annual C input rates largely exceed the realistic ranges from the literature for most soil types. The only soil types for which this scenario is realistic are the shallow soils (Calcaric Rendzic Leptosol and Hypereutric Epileptic Cambisol) and the sandy Dystric Cambisol, because these soils have lower SOC stocks than the others and are already close to their theoretical maximum SOC stocks.

The third scenario used realistic annual C input values from the literature, and found SOC accrual rates ranging from 0.32 – 1.04 tC ha^{-1} y^{-1} within the first 25 years. Examples can be found from previous studies of similar SOC accrual rates within decadal timescales following changes in land management strategies without changing the land use: transition from conventional to conservation agriculture in croplands (Autret *et al.*, 2016); promoting an increase in plant diversity in grasslands (Yang *et al.*, 2019); less frequent cutting in forests, or acting on forest productivity to increase root inputs and limiting soil disturbance during harvesting (Jandl *et al.*, 2007; Mayer *et al.*, 2020). The 1.5 tC ha^{-1} y^{-1} additional C inputs modelled in croplands resemble values calculated in a long-term field experiment after transition from conventional agriculture to conservation agriculture (1.72 tC ha^{-1} y^{-1} over 16 years, Autret *et al.*, 2016). Those inputs also correspond to what the model requires to maintain the theoretical maximum SOC stocks at steady state; this convergence confirms the robustness of the approach.

Using a percentile boundary line (here: 75th percentile of the SOC data) to estimate the theoretical maximum SOC stocks comes with a methodological challenge: the percentile regression necessarily depends on the size of the dataset and on its variability. A low percentile value within a large dataset underestimates the maximum SOC accrual, but an excessive percentile value within a small dataset produces an unrealistic target and increases the sensitivity to outliers. Other studies have used the following percentile values to estimate theoretical maximum SOC stocks at various spatial scales: Chen *et al.* (2019) compared maximum total SOC stocks following the 0.8, 0.85 and 0.9 percentile value at the national scale (1089 sites); Georgiou *et al.* (2022) compared the maximum mineral-associated SOC with low and high activity minerals at the 0.9, 0.95 and 0.975 percentiles at the global scale (1144 profiles). Standardized rules to define the choice of a percentile value for a target stock, depending on the scale of the study and the size and variability of the dataset, have yet to be established. Here, our choice of target SOC stocks at the 75th percentile is justified by the concordance between the annual C inputs necessary to maintain these stocks at steady state and realistic ranges of annual C inputs from Martin *et al.* (2021) and from regional Renecofor datasets (Table 2). By contrast, maintaining SOC stocks at the 88th percentile boundary line would require annual C inputs between 4.4 and 21.7 tC ha^{-1} y^{-1}, far in excess of what can be realistically added to soils. We recommend, where possible, to verify the realism of SOC stock targets using carbon dynamics models and matrix inversion to estimate the annual C inputs necessary to reach these targets in the long term.

Interrogating the realism of target SOC stocks is of particular importance when deeper soil horizons are considered. Another concept used to define target SOC stocks is to focus on the mineral associated carbon, considered to be more stable, by using the clay and fine silt fraction as a proxy of the amount of carbon that can be theoretically stored in a soil in the long term (Hassink 1997, Cotrufo *et al.*, 2019, Georgiou *et al.*, 2022). However, applying this concept over the whole soil profile leads to unrealistically high targets, and therefore unrealistic C inputs at depth (Appendix L).

Modelled SOC accrual in scenario 3 ranged from 8.5 to 26 tC ha^{-1} after 25 years, with a rapid decrease of SOC accrual rates with depth driven by decreasing C inputs. The deeper horizons of the soil provide limited opportunity for additional storage over short timescales using current land management practices. Furthermore, the proportion of new carbon inputs that is allocated to the fast carbon pool exceeds 85% at all depths in the soil profile (Appendix D): this implies that even in the deeper soil horizons, the majority of new C inputs is quickly mineralized, as also simulated by Sierra *et al.* (2024). The mean residence times (MRT) in the fast pool remain similar near the surface and at depth (17 – 38 years and 11 - 47 years respectively), but increase with depth in the slow pool (from 477 - 1100 years to 1744 - 5817 years). The greater contrast in mean residence times between the fast and slow pools at depth challenges our understanding of SOC dynamics.

Soil type did not play a major role on SOC accrual over short timescales: the observed differences in mineralization rates across soil types are not sufficient to have a significant impact after 25 years, especially in the fast pool (Appendix D). It is rather the land use that affects SOC accrual by controlling the quantity and vertical repartition of inputs (Appendix E). However, soil type has a strong influence on current SOC stocks by categorizing soils based on profile depth, rock fragment content and other physico-chemical properties. Hydromorphic soils in particular have total SOC stocks up to three times higher

than in other soil types, making their preservation particularly critical. These high SOC stocks are due to waterlogged conditions strongly limiting decomposers activity (Sahrawat, 2004), notably for energetic reasons (Keiluweit *et al.*, 2016).

Our model provides a widely-applicable tool to assess the effect of different soil types and initial distributions of SOC stocks on SOC dynamics at decadal timescales. It does not account for vertical transfer, but Balesdent et al (2018) showed that 13C incorporation in subsoil after a change in vegetation is slow and affects only long-term carbon dynamics. Sierra *et al.* (2024) also found that transport may only play a secondary role in the formation of soil carbon profiles according to simulation examples and measurements from carbon and radiocarbon profiles. Priming effect is not taken into consideration in our model, even though it is expected to occur when C inputs to the soil increase, which could cause simulated results to overestimate SOC accrual (Guenet *et al.*, 2018). Priming is difficult to include in predictive models because the processes involved are still poorly understood (Bernard *et al.*, 2022). Current explorations of the priming effect use either mechanistic models centred on microbial processes (Schimel, 2023), or theoretical models fitted to laboratory experiments, which do not fit the scope of our study.

Testing for the effect of temperature increase on mineralization rates led to an attenuation of SOC accrual by 2050 of 7 to 50 % depending on the climate scenario considered. We did not account holistically for the effects of climate change on SOC dynamics in this study: the combination of changes in temperature, CO_2 concentration and precipitation can drive a myriad of responses in net primary production, SOC input repartition and mineralization processes (Rocci *et al.*, 2021; Bruni *et al.*, 2021). In forests for instance, increased drought conditions may increase tree mortality, but might also enhance deeper roots prospection for water, thereby changing the vertical repartition of C inputs (Schlesinger *et al.*, 2016). Different soil types are also expected to respond differently to climate change, due for instance to the impact of soil texture on soil moisture regimes (Bormann, 2012; Hartley *et al.*, 2021). Here, we have considered a simplified case where humidity conditions do not change from the 2009-2019 period and dot not affect soil carbon dynamics. The scientific community needs to improve its understanding of the priming effect, of SOC dynamics processes driven by climate change, and to further explore how soil type influences organic matter decomposition dynamics over decadal timescales.

4.2: Implications for stakeholders: what levels of C accrual are achievable after 25 years?

Increasing soil organic carbon (SOC) stocks in soils has the potential to provide global benefits, but its successful implementation requires regional scale information on land use and soil type. An important aspect of this work is to provide relevant SOC storage targets to stakeholders. The maximum SOC accrual can be used as a theoretical, long-term target value, but is not representative of how much carbon can realistically be added to soils over decadal timescales. In the region of study, total SOC accrual after 25 years under a realistic scenario of C inputs was found to be five times lower than the maximum theoretical SOC accrual (0.57 MgC versus 2.5 MgC). Our simulation of rising temperatures following RCP4.5 (+1.0 °C) and RCP8.5 (+1.3°C) attenuated this SOC accrual by 7 - 38% and 10 - 50% respectively over 25 years through the increase of mineralization rates. This shows that increasing organic matter inputs to the soil remains worthwhile, since SOC accrual

remains significant even in an extreme scenario (highest projected increase in temperature but no change in humidity conditions).

Maps of SOC stocks are efficient tools to synthetize scientific results at the regional scale for stakeholders. Crucially, they highlight areas where soil degradation would lead to the greatest release of CO_2. The current SOC stocks have been built over timescales of centuries to millennia, especially in the deeper soil horizons, but can be rapidly lost due to land use change and other disturbances. Therefore, as highlighted by Sierra *et al.* (2024), the priority should be to preserve the existing SOC stocks, even as we attempt to implement innovative land management practices to maximize these SOC stocks where possible. Despite the high uncertainties associated with regional-scale estimations of SOC stocks (Appendix I-J), our mean SOC stock values of 87 tC ha-1 in the first 30 cm are in accordance with national-scale estimates that found SOC stocks of 75 – 100 tC ha^{-1} in the North-East of France (Pellerin *et al.*, 2021).

The map of maximum SOC accrual was found to be of limited interest because it does not provide a timescale for when that maximum SOC stock might realistically be reached. Reaching the theoretical maximum SOC stocks by the 2050 horizon for carbon neutrality would require prohibitively high annual C input rates. We therefore recommend maps of prospective SOC accrual to be time-specific, with C input rates within realistic ranges.

Our time-specific SOC accrual map is an improvement from simple representation of maximum theoretical SOC stocks, but remains a simplification of what can realistically be implemented. The map implies a uniform increase in C input rates for each land use in the entire region of study, but this would likely be hindered by practical and socio-economic factors. The SOC stock and time-specific SOC accrual maps should be used as part of a wider set of decision support tools for land planners. In some circumstances, adding organic carbon to soils might not even be the best solution for mitigating climate change: biomass harvest not returned to the soils can instead be used as a source of food, biosourced energy or biomaterials (Derrien *et al.*, 2023). These alternate uses of carbon biomass offer a mean of substituting fossil carbon, which should be verified quantitatively by life cycle analysis.

Finally, soil type information provided to stakeholders should not be limited to the current or prospective SOC stocks. Soil-type specific physico-chemical properties are an important but as of yet poorly considered factor for land planning. Soil type affects numerous soil functions such as water retention, resistance to erosion and nutrient cycling (Adhikari & Hartemink, 2016). These soil functions should be considered in addition to the SOC dynamics to choose management strategies adapted to each soil type.

5 Conclusion

Informing stakeholders on soil management strategies to preserve and maximize existing soil organic carbon (SOC) stocks is a pressing concern to the scientific community. It is critical to communicate on the effects of soil type, depth and land-use on SOC accrual in soil over time periods compatible with the roadmap for C neutrality, and to explore the C inputs necessary to reach these targets.

The annual C inputs necessary to reach theoretical maximum SOC stocks within 25 years in the region of study were found to exceed realistic C input ranges from the literature for most soil types (3.4 – 17.3 versus 1.18 – 6.8 tC ha^{-1} y^{-1}). The SOC accrual after 25 years modelled under a realistic scenario of increased C inputs was five times lower than the maximum SOC accrual estimated over the whole region of study (0.57 MgC versus 2.5 MgC).

We note a greater contrast of SOC mean residence times at depth, which invites further investigation: while a fraction of the new C inputs added to the deep soil horizons can remain stable over millennial timescales, the majority is mineralized within two decades. Simulating a rise in temperatures of 1.3°C over 25 years following RCP8.5 attenuated SOC accrual by 10 to 50%.

The effect of soil type on SOC mineralization rates was not visible over the decadal timescales considered. However, soil type plays an important role on the spatial repartition of the current SOC stocks that need to be preserved. Studies of SOC stocks and storage capacities should be complemented by more holistic explorations of soil functioning and ecosystem services.

This study provided a set of maps to give a more complete picture of the issues related to carbon storage in soils (carbon stocks, maximum SOC accrual, and realistic SOC accrual over decadal timescales). Such maps have the potential to facilitate communication with land planners and stakeholders by highlighting areas most worthy to preserve, and where carbon storage practices are likely to be the most efficient over decadal timescales. The efficacy of such maps as decision support tools should be explored via collaboration projects with stakeholders.

Author contributions

All authors have given approval to the final version of the manuscript. The manuscript was written through contributions of all authors as follows:

CHIROL Clémentine: Conceptualization; data analysis; SOC model development; original draft
SÉRÉ Geoffroy: Conceptualization; writing-review & editing
REDON Paul-Olivier: data provider; writing-review & editing
CHENU Claire: Conceptualization; writing-review & editing
DERRIEN Delphine: Conceptualization; SOC model advice and improvement; writing-review & editing

Declaration of competing interest

The authors declare that they have no known competing financial interests or personal relationships that could have appeared to influence the work reported in this paper.

Acknowledgements

We received funding from the ANDRA, DEEPSURF and LUE for this project. We would like to thank Dr. Catherine Galy and Dr. Paul-Olivier Redon (ANDRA) for providing datasets and information on the OPE study area; Line Boulonne (RMQS) and Manuel Nicolas and Sébastien Macé (Renecofor) for providing datasets; and Dr. Laurent Saint-André and Dr. Marie-Pierre Turpault for their advice on the project.

References

Abramoff, R.Z., Guenet, B., Zhang, H., Georgiou, K., Xu, X., Viscarra Rossel, R.A.,Yuan, W., Ciais, P. (2022). Improved global-scale predictions of soil carbon stocks with Millennial Version 2. Soil Biology and Biochemistry, 164, 108466. https://doi.org/10.1016/j.soilbio.2021.108466

Adhikari, K., & Hartemink, A. E. (2016). Linking soils to ecosystem services — A global review. Geoderma, 262, 101–111. https://doi.org/10.1016/j.geoderma.2015.08.009

Akpa, S. I., Odeh, I. O., Bishop, T. F., Hartemink, A. E., & Amapu, I. Y. (2016). Total soil organic carbon and carbon sequestration potential in Nigeria. Geoderma, 271, 202-215. https://doi.org/10.1016/j.geoderma.2016.02.021

Andriulo, A., Mary, B., & Guerif, J. (1999) Modelling soil carbon dynamics with various cropping sequences on the rolling pampas. Agronomie 19:365–377. https://doi.org/10.1051/agro:19990504

Angers, D. A., Arrouays, D., Saby, N. P. A., & Walter, C. (2011). Estimating and mapping the carbon saturation deficit of French agricultural topsoils: Carbon saturation of French soils. Soil Use and Management, 27(4), 448–452. https://doi.org/10.1111/j.1475-2743.2011.00366.x

Autret, B., Mary, B., Chenu, C., Balabane, M., Girardin, C., Bertrand, M., Grandeau, G., & Beaudoin, N. (2016). Alternative arable cropping systems: A key to increase soil organic carbon storage? Results from a 16 year field experiment. Agriculture, Ecosystems & Environment, 232, 150–164. https://doi.org/10.1016/j.agee.2016.07.008

Balesdent, J., Basile-Doelsch, I., Chadoeuf, J., Cornu, S., Derrien, D., Fekiacova, Z., & Hatté, C. (2018). Atmosphere–Soil Carbon Transfer as a Function of Soil Depth. Nature, 559(7715), 599–602. https://doi.org/10.1038/s41586-018-0328-3

Barré, P., Angers, D. A., Basile-Doelsch, I., Bispo, A., Cécillon, L., Chenu, C., Chevallier, T., Derrien, D., Eglin, T. K., & Pellerin, S. (2017). Ideas and perspectives: Can we use the soil carbon saturation deficit to quantitatively assess the soil carbon storage potential, or should we explore other strategies? Preprint Biogeosciences: Discussions. https://doi.org/10.5194/bg-2017-395

Beutler, S. J., Pereira, M. G., Tassinari, W. S., Menezes, M. D., Valladares, G. S., & dos Anjos, L. H. C. (2017). Bulk density prediction for Histosols and soil horizons with high organic matter content. Revista Brasileira de Ciência do Solo, 41(0). https://doi.org/10.1590/18069657rbcs20160158

Bormann, H. (2012). Assessing the soil texture-specific sensitivity of simulated soil moisture to projected climate change by SVAT modelling. *Geoderma*, *185*, 73-83. https://doi.org/10.1016/j.geoderma.2012.03.021

Bolinder, M. A., Janzen, H. H., Gregorich, E. G., Angers, D. A., & VandenBygaart, A. J. (2007). An approach for estimating net primary productivity and annual carbon inputs to soil for common agricultural crops in Canada. Agriculture, Ecosystems & Environment, 118(1-4), 29–42. https://doi.org/10.1016/j.agee.2006.05.013

Bruni, E., Guenet, B., Huang, Y., Clivot, H., Virto, I., Farina, R., ... & Chenu, C. (2021). Additional carbon inputs to reach a 4 per 1000 objective in Europe: Feasibility and projected impacts of climate change based on Century simulations of long-term arable experiments. Biogeosciences, 18(13), 3981-4004.

Chen, S., Arrouays, D., Angers, D. A., Chenu, C., Barré, P., Martin, M. P., Saby, N. P., & Walter, C. (2019). National estimation of soil organic carbon storage potential for arable soils: A data-driven approach coupled with carbon-landscape zones. Science of the Total Environment, 666, 355–367. https://doi.org/10.1016/j.scitotenv.2019.02.249

Clivot, H., Mary, B., Valé, M., Cohan, J.-P., Champolivier, L., Piraux, F., Laurent, F., & Justes, E. (2017). Quantifying in situ and modeling net nitrogen mineralization from soil organic matter in arable cropping systems. Soil Biology and Biochemistry, 111, 44–59. https://doi.org/10.1016/j.soilbio.2017.03.010

Cotrufo, M. F., Ranalli, M. G., Haddix, M. L., Six, J., & Lugato, E. (2019). Soil carbon storage informed by particulate and mineral-associated organic matter. Nature Geoscience, 12(12), 989–994. https://doi.org/10.1038/s41561-019-0484-6

Derrien, D., Barré, P., Basile-Doelsch, I., Cécillon, L., Chabbi, A., Crème, A., Fontaine, S., *et al.* (2023). Current controversies on mechanisms controlling soil carbon storage: Implications for interactions with practitioners and policy-makers. A review. Agronomy for Sustainable Development, 43(1), 21. https://doi.org/10.1007/s13593-023-00876-x

De Vos, B., Cools, N., Ilvesniemi, H., Vesterdal, L., Vanguelova, E., & Carnicelli, S. (2015). Benchmark values for forest soil carbon stocks in Europe: Results from a large scale forest soil survey. Geoderma, 251–252, 33–46. https://doi.org/10.1016/j.geoderma.2015.03.008

Dupouey, J. L., Cosserat, R., & Favre, F. (2008). Etablissement de la carte de l'utilisation ancienne des sols dans la première moitié du XIXe siècle sur le territoire de l'observatoire de Meuse/Haute Marne. In M. P. Turpault (Coord.), Caractérisation des milieux forestiers – site Andra Meuse/Haute-Marne, Rapport scientifique, Observatoire de l'écosystème forestier, HAVL-Programme observation et surveillance du stockage et de son environnement, ANDRA.

Fujita, Y., Witte, J. P. M., & van Bodegom, P. M. (2014). Incorporating microbial ecology concepts into global soil mineralization models to improve predictions of carbon and nitrogen fluxes. *Global biogeochemical cycles*, *28*(3), 223-238. https://doi.org/10.1002/2013GB004595

Georgiou, K., Jackson, R. B., Vindušková, O., Abramoff, R. Z., Ahlström, A., Feng, W., Harden, J. W., *et al.* (2022). Global stocks and capacity of mineral-associated soil organic carbon. Nature Communications, 13(1), 3797. https://doi.org/10.1038/s41467-022-31540-9

Guenet, B., Camino-Serrano, M., Ciais, P., Tifafi, M., Maignan, F., Soong, J. L., & Janssens, I. A. (2018). Impact of priming on global soil carbon stocks. Global Change Biology, 24, 1873–1883. https://doi.org/10.1111/gcb.14069

Guo, L. B., & Gifford, R. M. (2002). Soil carbon stocks and land use change: a meta analysis. Global change biology, 8(4), 345-360, https://doi.org/10.1046/j.1354-1013.2002.00486.x

Harrison, R. B., Footen, P. W., & Strahm, B. D. (2011). Deep soil horizons: Contribution and importance to soil carbon pools and in assessing whole-ecosystem response to management and global change. Forest Science, 57(1), 67–76. https://doi.org/10.1093/forestscience/57.1.67

Hartley, I. P., Hill, T. C., Chadburn, S. E., & Hugelius, G. (2021). Temperature effects on carbon storage are controlled by soil stabilisation capacities. Nature Communications, 12(1), 6713. https://doi.org/10.1038/s41467-021-27101-1

Hassink, J. (1997). The capacity of soils to preserve organic C and N by their association with clay and silt particles. Plant and Soil, 191, 77–87. https://doi.org/10.1023/A:1004213929699

Houot, S., Pons, M.-N., Pradel, M., Savini, I., & Tibi, A. (n.d.). Valorisation des matières fertilisantes d'origine résiduaire sur les sols à usage agricole ou forestier. INRA.

Jackson, R. B., Canadell, J., Ehleringer, J. R., Mooney, H. A., Sala, O. E., & Schulze, E. D. (1996). A global analysis of root distributions for terrestrial biomes. Oecologia, 108(3), 389–411. https://doi.org/10.1007/BF00333714

Jandl, R., Lindner, M., Vesterdal, L., Bauwens, B., Baritz, R., Hagedorn, F., ... Minkkinen, K. (2007). How strongly can forest management influence soil carbon sequestration? Geoderma, 137, 253–268. https://doi.org/10.1016/j.geoderma.2006.09.003

Jobbágy, E. G., & Jackson, R. B. (2000). The vertical distribution of soil organic carbon and its relation to climate and vegetation. Ecological Applications, 10(2), 423–436. https://doi.org/10.1890/1051-0761(2000)010[0423:TVDOSO]2.0.CO;2

Jreich, R. (2018). Vertical dynamics of soil carbon: Combined use of isotopic tracers and statistical meta-analysis (PhD thesis). Université Paris-Saclay.

Keiluweit, M., Nico, P. S., Kleber, M., & Fendorf, S. (2016). Are oxygen limitations under recognized regulators of organic carbon turnover in upland soils? Biogeochemistry, 127(2–3), 157–171. https://doi.org/10.1007/s10533-015-0180-6

Kögel-Knabner, I., & Amelung, W. (2021). Soil organic matter in major pedogenic soil groups. Geoderma, 384, 114785. https://doi.org/10.1016/j.geoderma.2020.114785

Lal, R. (2005). Forest soils and carbon sequestration. Forest Ecology and Management, 220(1–3), 242–258. https://doi.org/10.1016/j.foreco.2005.08.015

Levavasseur, F., Mary, B., Christensen, B. T., Duparque, A., Ferchaud, F., Kätterer, T., Lagrange, H., Montenach, D., Resseguier, C. & Houot, S. (2020). The simple AMG model accurately simulates organic carbon storage in soils after repeated application of exogenous organic matter. Nutrient Cycling in Agroecosystems, 117, 215–229. https://doi.org/10.1007/s10705-020-10065-x

Luo, Z., Feng, W., Luo, Y., Baldock, J., & Wang, E. (2017). Soil organic carbon dynamics jointly controlled by climate, carbon inputs, soil properties and soil carbon fractions. *Global change biology*, *23*(10), 4430-4439. https://doi.org/10.1111/gcb.13767

Malik, A. A., Puissant, J., Buckeridge, K. M., Goodall, T., Jehmlich, N., Chowdhury, S., ... Banfield, J. F. (2018). Land use driven change in soil pH affects microbial carbon cycling processes. Nature Communications, 9(1), 3591. https://doi.org/10.1038/s41467-018-05980-1

Mao, Z., Derrien, D., Didion, M., Liski, J., Eglin, T., Nicolas, M., Jonard, M., Saint-André, L. (2019). Modeling soil organic carbon dynamics in temperate forests with Yasso07. Biogeosciences, 16(9), 1955-1973. https://doi.org/10.5194/bg-16-1955-2019

Martin, M. P., Dimassi, B., Román Dobarco, M., Guenet, B., Arrouays, D., Angers, D. A., ... & Pellerin, S. (2021). Feasibility of the 4 per 1000 aspirational target for soil carbon: A case study for France. Global Change Biology, 27(11), 2458-2477. https://doi.org/10.1111/gcb.15547

Mathieu, J. A., Hatté, C., Balesdent, J., & Parent, É. (2015). Deep soil carbon dynamics are driven more by soil type than by climate: A worldwide meta-analysis of radiocarbon profiles. Global Change Biology, 21, 4278–4292. https://doi.org/10.1111/gcb.13012

Mayer, M., Prescott, C. E., Abaker, W. E., Augusto, L., Cécillon, L., Ferreira, G. W., ... Vesterdal, L. (2020). Influence of forest management activities on soil organic carbon stocks: A knowledge synthesis. Forest Ecology and Management, 466, 118127.

Minasny, B., Malone, B. P., McBratney, A. B., Angers, D. A., Arrouays, D., Chambers, A., ... Winowiecki, L. (2017). Soil carbon 4 per mille. Geoderma, 292, 59–86. https://doi.org/10.1016/j.geoderma.2017.01.002

Party, J. P., Vauthier, Q., & Rigou, L. (2019). Notice de la carte pédologique au 1/50000 de la zone OPE.

Pellerin, S., Bamière, L., Savini, I., Rechauchère, O., Launay, C., Martin, R., Schiavo, M., Angers, D., Augusto, L., Balesdent, J., Basile-Doelsch, I., Bellassen, V., Cardinael, R., Cécillon, L., Ceschia, E., Chenu, C., Constantin, J., Daroussin, J., Delacote, P., Delame, N., Gastal, F., Gilbert, D., Graux, A.-I., Guenet, B., Houot, S., Klumpp, K., Letort, E., Litrico, I., Martin, M., Menasseri-Aubry, S., Meziere, D., Morvan, T., Mosnier, C., Roger-Estrade, J., Saint-André, L., Sierra, J., Therond, O., Viaud, V., & Grateau, R., Le Perchec, S. (2021). Stocker du carbone dans les sols français.

Poeplau, C., Dechow, R., Begill, N., & Don, A. (2024). Towards an ecosystem capacity to stabilise organic carbon in soils. Global Change Biology, 30(8), e17453. https://doi.org/10.1111/gcb.17453

Rasmussen, C., Heckman, K., Wieder, W. R., Keiluweit, M., Lawrence, C. R., Berhe, A. A., ... Scow, K. M. (2018). Beyond clay: Towards an improved set of variables for predicting soil organic matter content. Biogeochemistry, 137(3), 297–306.

Rocci, K. S., Lavallee, J. M., Stewart, C. E., & Cotrufo, M. F. (2021). Soil organic carbon response to global environmental change depends on its distribution between mineral-associated and particulate organic matter: A meta-analysis. Science of the Total Environment, 793, 148569. https://doi.org/10.1016/j.scitotenv.2021.148569

Rowley, M. C., Grand, S., Spangenberg, J. E., & Verrecchia, E. P. (2021). Evidence linking calcium to increased organo-mineral association in soils. Biogeochemistry, 153(3), 223–241. https://doi.org/10.1007/s10533-021-00779-7

Saffih-Hdadi, K. & Mary, B. (2008). Modeling consequences of straw residues export on soil organic carbon. Soil Biol Biochem 40:594–607. https://doi.org/10.1016/j.soilbio.2007.08.022

Sahrawat, K. L. (2004). Organic matter accumulation in submerged soils. Advances in Agronomy, 81, 169–201.

Saxton, K. E., & Rawls, W. J. (2006). Soil water characteristic estimates by texture and organic matter for hydrologic solutions. Soil science society of America Journal, 70(5), 1569-1578. https://doi.org/10.2136/sssaj2005.0117

Schimel, J. (2023). Modeling ecosystem-scale carbon dynamics in soil: the microbial dimension. Soil Biology and Biochemistry, 178, 108948. https://doi.org/10.1016/j.soilbio.2023.108948

Schlesinger, W. H., Dietze, M. C., Jackson, R. B., Phillips, R. P., Rhoades, C. C., Rustad, L. E., & Vose, J. M. (2016). Forest biogeochemistry in response to drought. Global Change Biology, 22(7), 2318–2328. https://doi.org/10.1111/gcb.13105

Sierra, C. A., Ahrens, B., Bolinder, M. A., Braakhekke, M. C., von Fromm, S., Kätterer, T., ... Wang, G. (2024). Carbon sequestration in the subsoil and the time required to stabilize carbon for climate change mitigation. Global Change Biology, 30(1), e17153.

Six, J., Conant, R. T., & Paul, E. A. (2002). Stabilization mechanisms of soil organic matter: Implications for C-saturation of soils. Plant and Soil, 241(1), 155–176. https://doi.org/10.1023/A:1016125726789

Shiri, J., Keshavarzi, A., Kisi, O., Karimi, S., & Iturraran-Viveros, U. (2017). Modeling soil bulk density through a complete data scanning procedure: Heuristic alternatives. Journal of Hydrology, 549, 592-602. https://doi.org/10.1016/j.jhydrol.2017.04.035

Tautges, N. E., Chiartas, J. L., Gaudin, A. C. M., O'Geen, A. T., Herrera, I., & Scow, K. M. (2019). Deep soil inventories reveal that impacts of cover crops and compost on soil carbon sequestration differ in surface and subsurface soils. Global Change Biology, 25(11), 3753–3766. https://doi.org/10.1111/gcb.14762

Verma, Y., Singh, N. K., & Pathak, S. O. (2017). Application of carbon isotopic techniques in the study of soil organic matter dynamics. International Journal of Chemical Studies, 5(6), 1123–1128.

Wiesmeier, M., Von Lützow, M., Spörlein, P., Geuß, U., Hangen, E., Reischl, A., ... Kögel-Knabner, I. (2015). Land use effects on organic carbon storage in soils of Bavaria: The importance of soil types. Soil and Tillage Research, 146, 296–302. https://doi.org/10.1016/j.still.2014.10.003

Yang, Y., Tilman, D., Furey, G., & Lehman, C. (2019). Soil carbon sequestration accelerated by restoration of grassland biodiversity. Nature Communications, 10(1), 718. https://doi.org/10.1038/s41467-019-08636-w

Appendices

Appendix A: List of soil properties collected at each soil profile and their measurement protocol

Study type	Soil Property	Unit	Method
Field observation	Slope	%	In situ operator's assessment
	Soil depth	Cm	In situ operator's assessment
	Horizon Textural Class	Type	In situ operator's assessment completed by NF X 31-107
	Horizon Compacity	Type	knife test (ISO 25177: 2008)
	Horizon Rock Fragment Content	%	In situ operator's assessment
	Horizon Hydromorphic Features	Type	In situ operator's assessment
Lab Agronomical Analysis	Horizon pH	-	NF ISO 10390
	Horizon OM	g/kg	NF ISO 10694
	Horizon CaCO3	g/kg	NF ISO 10693

Appendix B: List of descriptors used to plot the SOC content curves for each soil type and land use: Ω_1 the SOC content of the soil type at maximal depth, Ω_2 the SOC content at the surface, and Ω_3 the depth at half maximum of the SOC content (based on Mathieu *et al.* (2015) and Jreich (2018))

Land use	Soil type (WRB)	Soil type (RPF)	Ω_1 Bottom SOC (g/kg)	Ω_2 Top SOC (g/kg)	Ω_3 Depth at half maximum of the carbon content (cm)
Cropland	Calcaric rendzic leptosol	Rendosol	17	31	17
Forest	Calcaric rendzic leptosol	Rendosol	22	74	16
Grassland	Calcaric rendzic leptosol	Rendosol	12	53	15
Cropland	Calcaric cambisol	Calcosol	14	33	21
Forest	Calcaric cambisol	Calcosol	17	62	18
Grassland	Calcaric cambisol	Calcosol	14	54	15
Cropland	Hypereutric epileptic cambisol	Rendisol	19	38	13
Forest	Hypereutric epileptic cambisol	Rendisol	16	60	12
Cropland	Hypereutric cambisol	Calcisol	10	24	17
Forest	Hypereutric cambisol	Calcisol	22	64	21
Grassland	Hypereutric cambisol	Calcisol	14	54	15
Cropland	Eutric cambisol	Brunisol	8	18	21

Forest	Eutric cambisol	Brunisol	8	45	16
Grassland	Eutric cambisol	Brunisol	5	23	21
Forest	Dystric cambisol	Alocrisol	4	31	15
Cropland	Stagnosol	Rédoxisol	10	21	19
Forest	Stagnosol	Rédoxisol	9	46	17
Grassland	Stagnosol	Rédoxisol	9	40	14
Cropland	Gleysol	Réductisol	16	26	16
Grassland	Gleysol	Réductisol	21	68	18

Appendix C: Details of model functioning

A depth-dependent SOC dynamic model using multilayer soil modules was built to establish the time needed to reach different levels of carbon storage in the soil. SOC is allocated to three boxes (fast, slow, stable) corresponding to different SOC mineralization rates defined by Balesdent *et al.* (2018) based on a meta-analysis of changes in stable carbon isotope signatures at 55 grassland, forest and cropland sites, in the tropical zone.

The mineralization factors associated with each box were then corrected for temperate soils using correction factors defined for the AMG model to account for the difference in environmental conditions (temperature and humidity) between tropical and temperate, but also to account for the differences in pH, clay content and $CaCO_3$ between soil types. The correction factors linked to temperature and humidity are based on Andriulo *et al.* (1999) and Saffih-Hdadi and Mary (2008). The correction factors linked to pH, clay content and $CaCO_3$ were previously established by Clivot *et al.* (2017) based on the monitoring of N mineralization in 65 bare fallow soils representative of arable cropping systems in France, over a depth up to 150cm. These corrections are in accordance with recommendations from Rasmussen *et al.* (2018), for whom SOM stabilization not only depends on clay content, but also on pH and exchangeable calcium for alkaline soils. The correction factors for the temperature (T), humidity (H), clay content (A), pH and $CaCO_3$, as used in the 2019 AMG model, were as follows:

- $fT = \frac{25}{1+(25-1)*\ e^{0.12*15}*e^{-0.12*\mathrm{T}}}$ *[Equation C1]*
- $fH = \frac{1}{1+0.03*e^{-5.247*(\mathrm{P}-\mathrm{PET})/1000}}$ *[Equation C2]*
- $fA = e^{-2.519*10^{-3}*\mathrm{Clay}}$ *[Equation C3]*

- $fpH = e^{-0.112 * (\mathrm{pH}-8.5)^2}$ *[Equation C4]*
- $fCaCO_3 = \frac{1}{1+(1.5*10^{-3} * \mathrm{CaCO3})}$ *[Equation C5]*

With T the mean annual temperature, P the mean annual precipitation and PET the potential evapotranspiration.

The total correction factor f = fT * fH * fA * fpH * $fCaCO_3$, was calculated for the tropical sites from Balesdent *et al.* (2018) and for the temperate conditions in the OPE region of the study (f_{BAL} and f_{OPE} respectively). The corrected mineralization factors $k1_{corr}$ and $k2_{corr}$ were obtained with the following equations:

- $k1_{corr} = k1 * f_{OPE} / f_{BAL}$ *[Equation C6]*
- $k2_{corr} = k2 * f_{OPE} / f_{BAL}$ *[Equation C7]*

For each soil type and land use, the initial carbon stocks every 10 cm was again obtained by data interpolation with the Jreich method (2018); they were distributed between the three pools based on the depth-dependent allocation factors defined by Balesdent *et al.* (2018), as follows:

- $C1_{init}(i) = C_{init}(i) * a1(i)$ *[Equation C8]*
- $C2_{init}(i) = C_{init}(i) * a2(i)$ *[Equation C9]*
- $C3_{init}(i) = C_{init}(i) * (1-(a1(i)+a2(i)))$ *[Equation C10]*

With C_{init} the initial carbon stock, and a1 and a2 the proportion of carbon in pool 1 and 2 at each depth i.

The incorporated soil carbon inputs at each depth i and timestep t were added as follows:

- $C1_{in}(t,i) = INPUT(i) * \alpha(i)$ *[Equation C11]*
- $C2_{in}(t,i) = INPUT(i) * (1-\alpha(i))$ *[Equation C12]*

with α the proportion of new carbon inputs that is allocated to the fast carbon pool, calculated from the steady-state input equations (see Equations C19-22 below).

The outputs at each timestep were a function of the carbon stock at timestep t and of the corrected mineralization factors at each depth i, as follows:

- $C1_{out}(t,i)=C1(t,i) * (e^{-k1_{corr}(i)*\mathrm{timestep}} - 1)$ *[Equation C13]*
- $C2_{out}(t,i)=C2(t,i) * (e^{-k2_{corr}(i)*\mathrm{timestep}} - 1)$ *[Equation C14]*

The change in soil carbon stock at each depth i between t and t+1 was defined as follows:

- $dC1(t,i)=C1_{out}(t,i) + C1_{in}(t,i)$ *[Equation C15]*
- $dC2(t,i)=C1_{out}(t,i) + C2_{in}(t,i)$ *[Equation C16]*

The soil carbon stocks at t+1 were therefore defined as:

- $C1(t+1,i) = C1(t,i) + dC1(t,i)$ *[Equation C17]*
- $C2(t+1,i) = C2(t,i) + dC2(t,i)$ *[Equation C18]*

The corrected mineralization rates also led to the definition of carbon mean residence times as a function of depth for each soil type (MRT = 1/k, see Appendix B). SOC mean residence times at the steady state depend on the physico-chemical properties of the studied soil types: in our study site, they range from 50 – 100 years in the topsoil and from 145 – 453 years underneath. The model was initialized under the assumption that the carbon stocks calculated at the different depths in 2018 were at steady state. This assumption is justified on average by a land occupation map from 1830 showing limited changes in land use over the past 200 years (Dupouey *et al.*, 2008). Inversing the model at the steady state yielded the vertical repartition of yearly C inputs necessary to keep the input and output fluxes equal across the full profile. We defined $INPUT_{eq}$ the repartition of incorporated C inputs every 10 cm at the steady state, as follows:

- $C1_{eq}(i) = INPUT(i) * \frac{\alpha(i)}{k1_{corr}}$ *[Equation C19]*
- $C2_{eq}(i) = INPUT(i) * \frac{(1-\alpha)}{k2_{corr}}$ *[Equation C20]*

The two previous equations are used to define α as follows:

- $\alpha(i) = \frac{\frac{a1*k1corr}{a2*k2corr}}{1+(\frac{a1*k1corr}{a2*k2corr})}$ *[Equation C21]*

This estimate of the yearly inputs did not distinguish between surface inputs and inputs by the root systems. The model further assumed that there was no vertical redistribution of SOC between the layers following this initial allocation (Balesdent *et al.*, 2018). Then, the allocation and mineralization rates of these inputs were used at each depth layer to infer the mean residence time of the C inputs per land use: this second definition of the mean residence time depends on both the physico-chemical properties of the soil and on the vertical repartition of inputs.

Appendix D: Details of the SOC average mean residence time (MRT = 1/k) in the fast pool ($MRT_1 = 1/k_1$) and in the slow pool ($MRT_2 = 1/k_2$), represented in years as a function of depth for each soil type, using parameters from Balesdent *et al.* (2018), with correction factors from the AMG model for the temperature, P/PET, pH, clay content and $CaCO_3$. a1 and a2 are the proportion of initial C at steady state distributed in the fast and slow pools – the carbon proportion in the inert pool being the complement to reach one). α represents the proportion of new carbon inputs that is allocated to the fast carbon pool (see Equation C21), the complement is allocated to the slow pool, no carbon is allocated to the inert pool. Soil 1: Calcaric rendzic leptosol, soil 2: Calcaric cambisol; soil 3: Hypereutric epileptic cambisol; soil 4: Hypereutric cambisol; soil 5: Eutric cambisol; soil 6: Dystric cambisol; soil 7: Stagnosol; soil 8: Gleysol.

Depth (cm)	a1	a2	α	Mean Residence Time MRT (y)															
				Soil 1		Soil 2		Soil 3		Soil 4		Soil 5		Soil 6		Soil 7		Soil 8	
				MRT1	MRT2	MRT1	MRT2	MRT1	MRT2	MRT1	MRT2	MRT1	MRT2	MRT1	MRT2	MRT1	MRT2	MRT1	MRT2
0-10	0,61	0,34	0.98	22	628	20	563	22	630	20	566	26	742	38	1100	23	664	17	477
10-20	0,29	0,67	0.92	31	777	27	696	31	779	28	701	36	918	37	948	32	822	23	591
20-30	0,11	0,85	0.86	13	643	14	676	26	1284	23	1121	29	1422	24	1190	21	1031	15	741
30-40	0,07	0,86	0.86	13	863	13	908	25	1724	22	1505	28	1910	25	1727	14	977	13	892
40-50	0,07	0,83	0.88			11	1013	26	2321	23	2026	29	2571	22	1943	15	1315	14	1200
50-60	0,07	0,80	0.90			13	1317			44	4654	30	3198	24	2526	16	1710	15	1561
60-70	0,07	0,75	0.91							47	5171	32	3553	25	2807	17	1900	16	1734
70-80	0,05	0,71	0.91							42	5817	29	3997	23	3158	14	1948	14	1951
80-90	0,04	0,65	0.91							37	5817	26	3997	20	3158	12	1948	11	1744
90-100	0,04	0,60	0.92											22	3501	12	1948	11	1744
Average MRT above 30 cm				62		57		69		62		81		100		70		50	
Average MRT below 30 cm				145		155		309		453		418		384		226		206	

Appendix E: Vertical repartition in % of yearly C inputs at the steady state for each soil type, land use and depth layer every 10 cm. The bottom of the table provides the total inputs in tC ha^{-1} y^{-1} needed to stay at the steady state, or to reach the maximum SOC stocks estimated by the 75th percentile data-driven method. C = Cropland; F = Forest; G = Grassland.

Depth (cm)	Calcaric rendzic leptosol			Calcaric cambisol			Hypereutric epileptic cambisol		Hypereutric cambisol			Eutric cambisol			Dystric cambisol	Stagnosol			Gleysol	
	C	F	G	C	F	G	C	F	C	F	G	C	F	G	F	C	F	G	C	G
0	0.672	0.709	0.737	0.701	0.700	0.764	0.739	0.772	0.705	0.699	0.743	0.668	0.738	0.760	0.629	0.499	0.651	0.630	0.489	0.606
10	0.173	0.167	0.158	0.148	0.155	0.128	0.184	0.172	0.164	0.171	0.154	0.160	0.157	0.151	0.174	0.130	0.149	0.142	0.108	0.141
20	0.116	0.096	0.082	0.082	0.083	0.060	0.045	0.034	0.054	0.055	0.046	0.061	0.049	0.045	0.061	0.066	0.060	0.060	0.056	0.061
30	0.039	0.028	0.023	0.033	0.031	0.023	0.030	0.020	0.032	0.032	0.025	0.037	0.023	0.020	0.025	0.058	0.041	0.044	0.043	0.037
40				0.020	0.018	0.014	0.003	0.002	0.024	0.023	0.018	0.023	0.012	0.010	0.019	0.047	0.026	0.030	0.038	0.026
50				0.015	0.013	0.011			0.008	0.007	0.005	0.017	0.008	0.005	0.013	0.038	0.017	0.021	0.033	0.019
60									0.007	0.006	0.005	0.015	0.006	0.004	0.011	0.034	0.013	0.017	0.030	0.016
70									0.006	0.005	0.004	0.013	0.005	0.003	0.009	0.030	0.010	0.014	0.026	0.013
80									0.002	0.002	0.001	0.006	0.002	0.001	0.009	0.029	0.009	0.013	0.028	0.013
90															0.008	0.027	0.009	0.012	0.027	0.013
100															0.009	0.030	0.010	0.013	0.031	0.014
110															0.009	0.012	0.004	0.005	0.031	0.014
120															0.009				0.031	0.014
130															0.009				0.028	0.013
140															0.009					
Total inputs to stay at the steady state (tC ha^{-1} y^{-1})	1.34	2.75	1.91	1.84	2.83	2.73	1.47	1.97	1.36	2.26	2.51	0.98	2.02	1.19	1.03	1.50	2.33	1.92	2.79	4.59
Total inputs to reach Max SOC (tC ha^{-1} y^{-1})	3.15	3.61	2.20	3.14	2.26	1.44	3.22	5.99	3.15	3.61	2.20	3.14	2.26	1.44	3.22	5.99	3.15	3.61	2.20	3.14

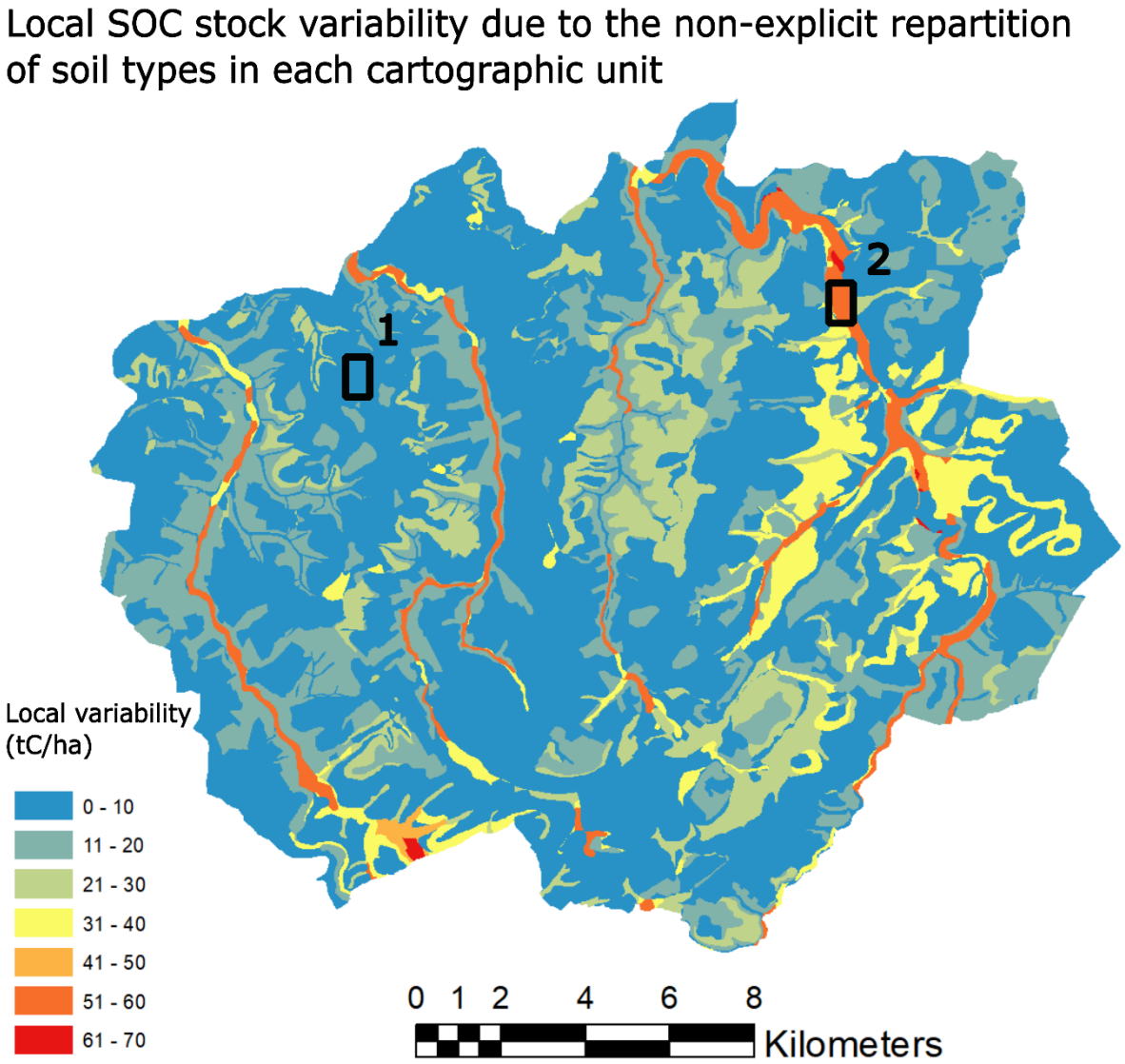

Appendix F: Local uncertainty of SOC linked to the non-explicit repartition of soil types within the cartographic units. As an example, in zone 1, which is under forest, the represented soil types are 80% Eutric cambisol (157 tC ha^{-1}) and 20% Stagnosol (172 tC ha^{-1}). In zone 2, which is under grassland, the represented soil types are 80% Stagnosol (161 tC ha^{-1}) and 20% Gleysol (333 tC ha^{-1}). For this reason, the local variability of SOC stocks is higher in zone 2 than zone 1.

Appendix G: SOC stocks and maximum storage capacity above and below 30 cm (below 30 cm represented in bold)

	Median SOC stocks in 2018 (tC ha^{-1})			**Theoretical maximum SOC stocks (75th percentile)**	**Theoretical maximum SOC stocks (88th percentile)**	**Maximum SOC accrual (tC ha^{-1})**		
	Cropland	Grassland	Forest	All land uses	All land uses	Cropland	Grassland	Forest
Calcaric Rendzic Leptosol	70 **8**	155 **12**	138 **11**	155 **12**	170 **13**	85 **5**	60 **6**	17 **2**
Calcaric Cambisol	81 **19**	155 **36**	123 **24**	155 **36**	180 **42**	75 **17**	41 **16**	32 **12**
Hypereutric Epileptic Cambisol	78 **14**	112 **17**	97 **10**	112 **17**	122 **18**	34 **3**		15 **7**
Hypereutric Cambisol	63 **40**	142 **86**	104 **56**	142 **86**	180 **109**	78 **46**	28 **32**	38 **30**
Eutric Cambisol	59 **43**	130 **64**	119 **38**	130 **64**	146 **72**	71 **22**	59 **45**	11 **27**
Dystric Cambisol		101 **68**	76 **44**	101 **68**	117 **79**			25 **24**
Stagnosol	64 **101**	142 **143**	76 **44**	142 **143**	180 **182**	76 **42**	50 **74**	28 **85**
Gleysol	78 **202**	187 **289**	114 **58**	187 **289**	209 **324**	110 **87**	32 **111**	

Appendix H: simulated SOC accrual in tC ha^{-1} in the different soil types and land uses (C= cropland, F=forest, G=grassland) after 1, 10, 50, 200, 1000 and 5000 years of model run under a scenario of additional inputs of 0.5 tC ha^{-1} y^{-1} under forests, 1.0 tC ha^{-1} y^{-1} under grasslands and 1.5 tC ha^{-1} y^{-1} under croplands. Constant temperature in the top part of the table.

Years	Calcaric rendzic leptosol			Calcaric cambisol			Hypereutric epileptic cambisol		Hypereutric cambisol			Eutric cambisol			Dystric Cambisol	Stagnosol			Gleysol	
	C	G	F	C	G	F	C	F	C	G	F	C	G	F	F	C	G	F	C	G
1	1.5	1.0	0.5	1.5	1.0	0.5	1.5	0.5	1.5	1.0	0.5	1.5	1.0	0.5	0.5	1.5	1.0	0.5	1.5	1.1
10	12.6	8.6	4.6	12.5	8.6	4.6	12.9	4.6	12.6	8.7	4.5	13.1	8.8	4.6	4.6	12.8	8.8	4.6	12.3	8.9
25	**23.7**	**16.2**	**8.7**	**22.9**	**15.8**	**8.4**	**24.5**	**8.6**	**23.7**	**16.2**	**8.5**	**26.0**	**17.3**	**9.1**	**9.4**	**23.6**	**16.4**	**8.7**	**21.3**	**15.5**
50	32.6	22.2	11.9	30.6	21.0	11.2	34.3	11.9	32.2	21.9	11.5	37.5	24.8	13.0	14.4	33.1	23.1	12.2	27.6	20.1
100	39.1	26.3	14.0	36.0	24.4	13.0	40.9	14.0	38.2	25.7	13.5	46.5	30.3	15.9	18.8	40.6	27.9	14.6	32.7	23.3
200	45.5	30.0	16.0	41.8	27.8	14.9	46.7	15.7	44.2	29.4	15.4	54.0	34.5	18.0	22.1	49.1	32.7	16.8	40.1	27.6
5000	84.5	52.1	27.4	78.9	48.4	26.4	92.4	27.6	98.5	60.1	32.1	133.8	69.6	36.2	50.0	142.3	77.9	36.1	118.5	64.1
	SOC accrual after 25 years under temperature increase of 1.0 °C by 2050 (RCP 4.5 scenario)																			
25	**21.5**	**13.6**	**5.5**	**20.2**	**12.5**	**5.3**	**22.1**	**6.2**	**21.4**	**13.0**	**5.8**	**24.1**	**15.5**	**6.5**	**8.0**	**21.3**	**13.8**	**5.9**	**17.8**	**10.5**
	SOC accrual after 25 years under temperature increase of 1.3 °C by 2050 (RCP 8.5 scenario)																			
25	20.8	12.9	4.5	19.4	11.4	4.3	21.4	5.5	20.7	12.1	5.0	23.5	14.9	5.8	7.5	20.5	13.0	5.1	16.7	9.0

765

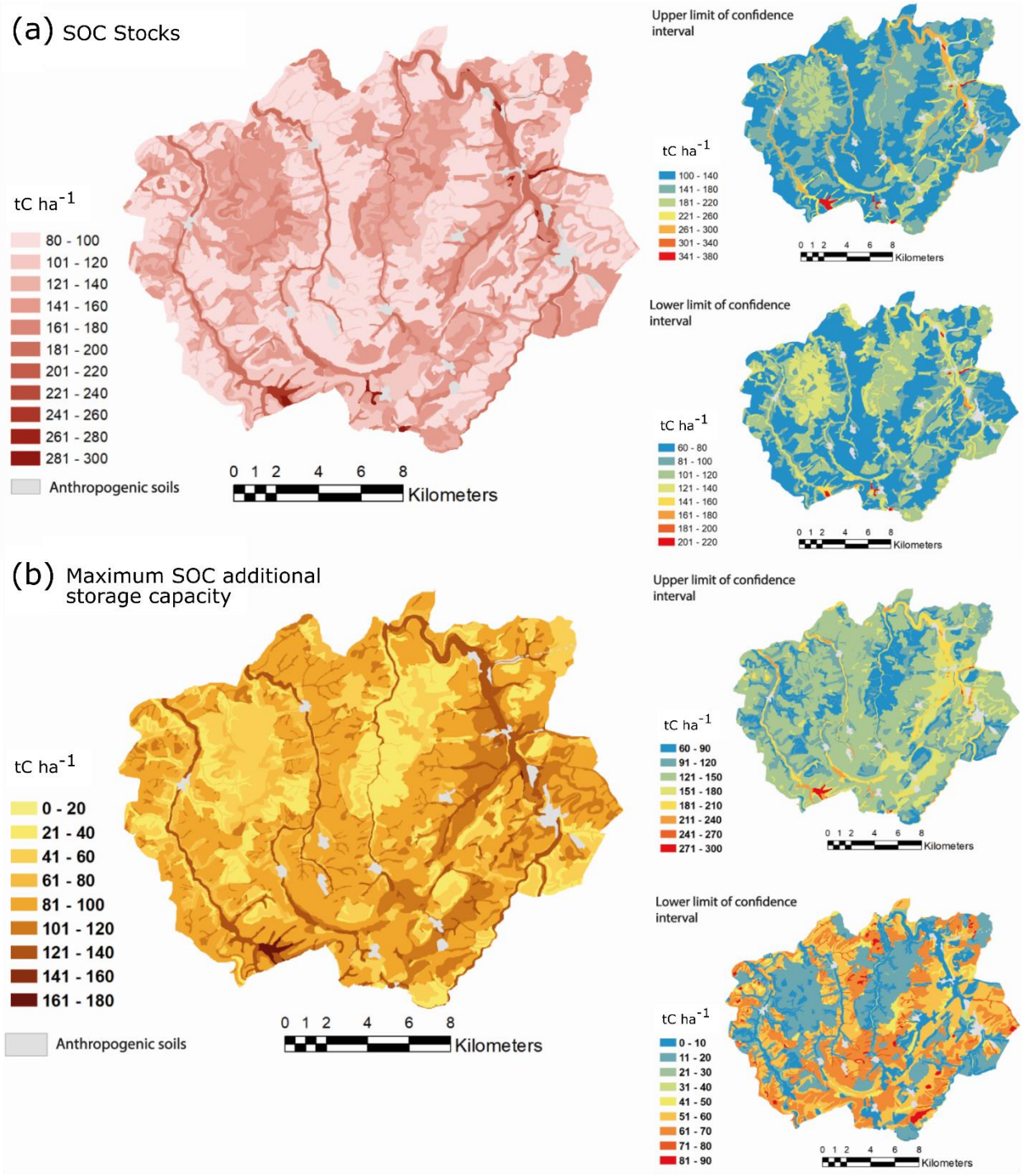

Appendix I: SOC stocks and maximum SOC additional storage capacity, with lower and upper confidence intervals as estimated by the bootstrap method. The SOC stock in the region of study ranges from 2.4 – 5.3 MtC and the maximum SOC additional storage capacity 1.2 - 4.1 MtC.

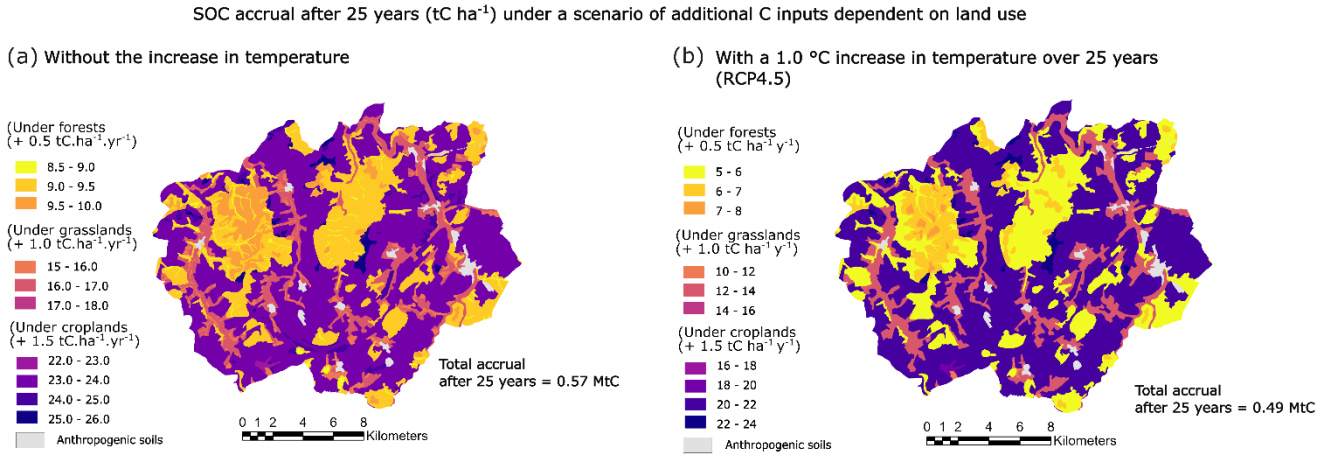

Appendix J: SOC accrual after 25 years under a scenario of additional C inputs dependent on land use, (a) with temperatures staying at their 2018 level, and (b) with a 1.0 °C increase in temperature over 25 years, increasing the C mineralization rates according to the correction factors of the AMG model. The attenuation in SOC accrual due to increased mineralization rates is (0.49 – 0.57) / 0.57 = 14%. The 1.0 °C increase in temperature was obtained from model simulations of mean annual temperatures by the Meteo France ALADIN63_CNRM-CM5 model under scenario RCP4.5, within an 8 km radius area around Bure (55087), comparing the year intervals 2046-2055 and 2009-2019. Source: Drias, données Météo-France, CERFACS, IPSL.

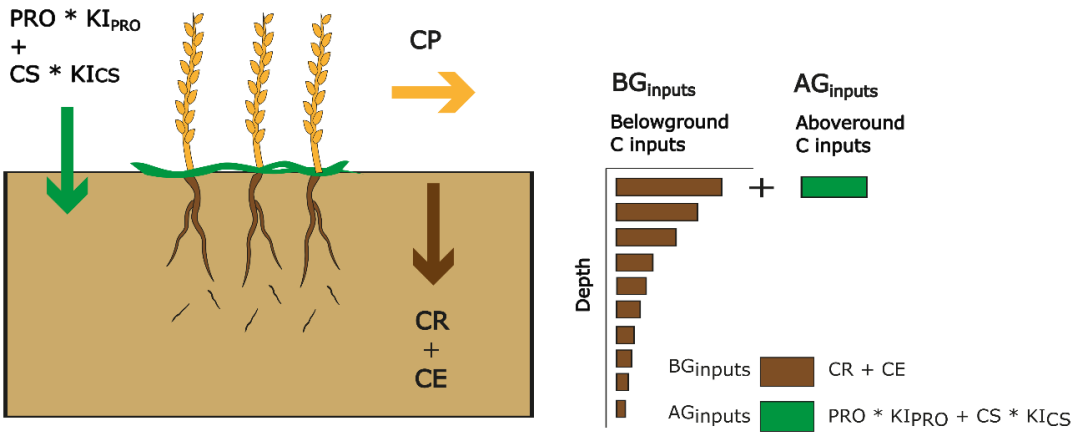

CE = extra-root C (C content in roots * 0.65)
CP = C product (crop yield * C content in plant parts)
CR = C roots (CP * Root:Shoot ratio / Harvest Index)
CS = C straw (CP * (1 - Harvest Index) / Harvest Index)
KI_{CS} = coefficient of incorporation for the straw (0.1, Girard et al., 2011)
KI_{PRO} = coefficient of incorporation for the organic amendments (0.3, Girard et al., 2011)
PRO = Organic amendments from manure * organic matter content in manure * C content in organic matter

C content in plant parts = 0.45 (Bolinder et al., 2007)
Harvest Index = 0.4 (Bolinder et al., 2007)
Organic matter content in manure = 0.57 (INRAE - MAFOR)
Root:Shoot ratio = 0.1 in croplands (Jackson et al., 1996)

Appendix K: Estimation of the current incorporated C inputs in croplands via a yield-based allocation coefficients method from Bolinder *et al.* (2017) using agricultural yield and amendment values based on compiled reports from 2010-2019 in the region of study. The allocation coefficients were derived from the literature (harvest index and carbon content in plant parts from Bolinder *et al.* (2007), organic matter content in manure from Houot *et al.* (2014), root:shoot ratios in croplands from Jackson *et al.* (1996), incorporation coefficients form Girard *et al.* (2011)). Estimated C inputs in the croplands in the region of study are 1.4tC ha^{-1} y^{-1}, with a mean winter wheat yield value of 5.53 tDM ha^{-1} y^{-1} and an amendment value of 2.13 tDM ha^{-1} y^{-1}. The average C inputs at the steady state obtained via model inversion in the croplands of the region of study, weighted by the proportion of each soil type in the cropland areas, amount to 1.7 tC ha^{-1} y^{-1}.

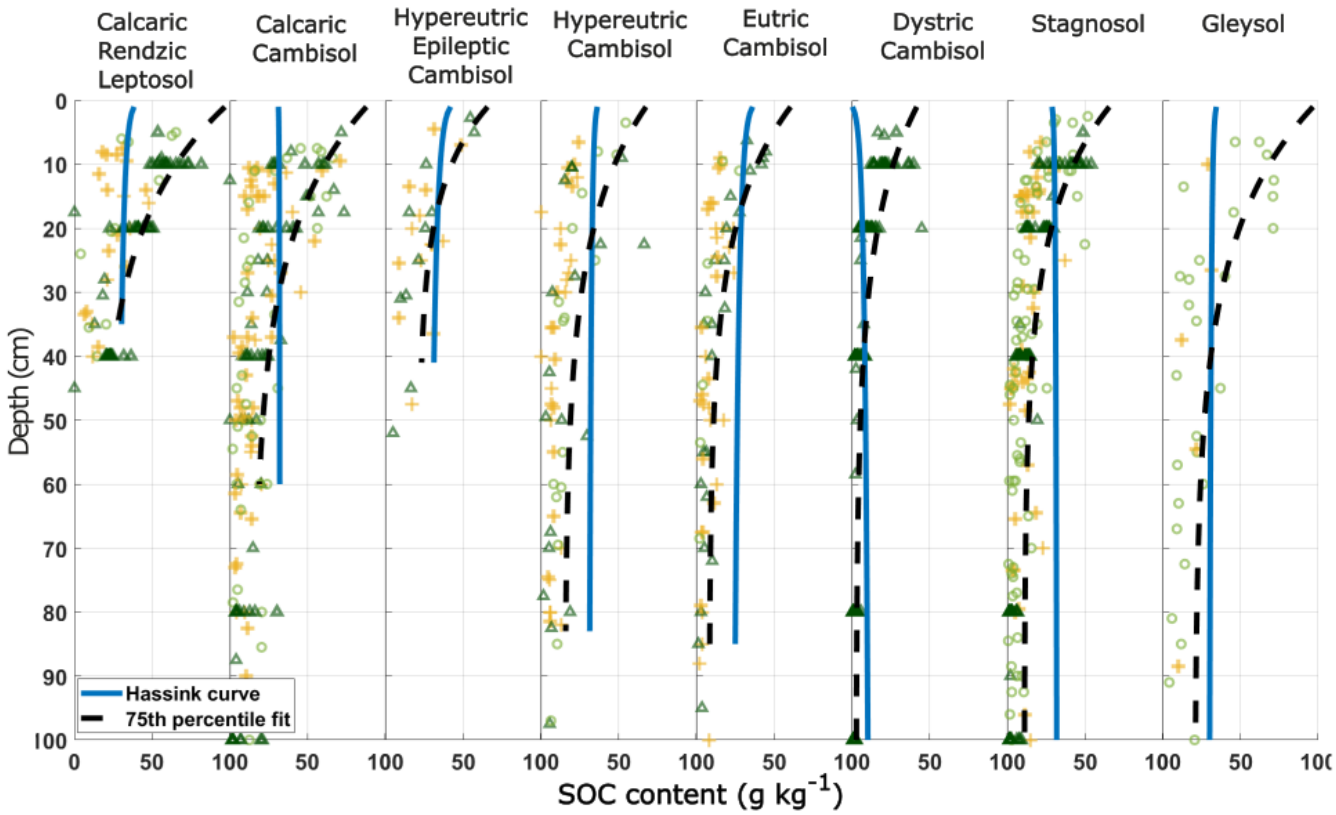

Appendix L: Carbon saturation curves from Hassink as a function of depth. The Hassink equation was established empirically on the basis of 20 Dutch grassland soils considered to be at the stationary state, as follows: C_{sat} = 4.09 +0.37 * (Clay + fineSilt) (%) where C_{sat} is the theoretical carbon saturation concentration in the fine fraction in g kg^{-1}. The Hassink equation provides unrealistic profiles of maximum SOC content distribution in the fine fraction at depth below 30 cm, especially in the Hypereutric Cambisol, Eutric Cambisol and Stagnosol, as the equation only accounts for soil texture and does not consider the biotic controls on C inputs and SOC decomposition rates. As comparison, the 75th percentile fit represents a theoretical maximum SOC content in both the fine fraction and the particulate organic matter.